The Astrophysical Journal Supplement Series, 235:42 (19pp), 2018 April https://doi.org/10.3847/1538-4365/aa9e8a

The Fourteenth Data Release of the Sloan Digital Sky Survey: First Spectroscopic Data from the Extended Baryon Oscillation Spectroscopic Survey and from the Second Phase of the Apache Point Observatory Galactic Evolution Experiment

Bela Abolfathi[1], D. S. Aguado[2,3], Gabriela Aguilar[4], Carlos Allende Prieto[2,3], Andres Almeida[5], Tonima Tasnim Ananna[6], Friedrich Anders[7], Scott F. Anderson[8], Brett H. Andrews[9], Borja Anguiano[10], Alfonso Aragón-Salamanca[11], Maria Argudo-Fernández[12], Eric Armengaud[13], Metin Ata[7], Eric Aubourg[14], Vladimir Avila-Reese[4], Carles Badenes[9], Stephen Bailey[15], Christophe Balland[16], Kathleen A. Barger[17], Jorge Barrera-Ballesteros[18], Curtis Bartosz[8], Fabienne Bastien[19,44], Dominic Bates[20], Falk Baumgarten[7,21], Julian Bautista[22], Rachael Beaton[23], Timothy C. Beers[24], Francesco Belfiore[25,26,27], Chad F. Bender[28], Mariangela Bernardi[29], Matthew A. Bershady[30], Florian Beutler[31], Jonathan C. Bird[32], Dmitry Bizyaev[33,34,35], Guillermo A. Blanc[23,108], Michael R. Blanton[36], Michael Blomqvist[37], Adam S. Bolton[38], Médéric Boquien[12], Jura Borissova[39,40], Jo Bovy[41,42,133], Christian Andres Bradna Diaz[43], William Nielsen Brandt[19,44,45], Jonathan Brinkmann[33], Joel R. Brownstein[22], Kevin Bundy[27], Adam J. Burgasser[46], Etienne Burtin[13], Nicolás G. Busca[14], Caleb I. Cañas[44], Mariana Cano-Díaz[47,136], Michele Cappellari[48], Ricardo Carrera[2,3], Andrew R. Casey[49], Bernardo Cervantes Sodi[50], Yanping Chen[51], Brian Cherinka[52], Cristina Chiappini[7], Peter Doohyun Choi[53], Drew Chojnowski[34], Chia-Hsun Chuang[7], Haeun Chung[54], Nicolas Clerc[55,56,57], Roger E. Cohen[58,59], Julia M. Comerford[60], Johan Comparat[55], Janaina Correa do Nascimento[61,62], Luiz da Costa[62,63], Marie-Claude Cousinou[64], Kevin Covey[65], Jeffrey D. Crane[23], Irene Cruz-Gonzalez[4], Katia Cunha[28,63], Gabriele da Silva Ilha[62,66], Guillermo J. Damke[10,67,68], Jeremy Darling[60], James W. Davidson, Jr.[10], Kyle Dawson[22], Miguel Angel C. de Icaza Lizaola[4], Axel de la Macorra[69], Sylvain de la Torre[37], Nathan De Lee[70,32], Victoria de Sainte Agathe[71], Alice Deconto Machado[62,66], Flavia Dell'Agli[2,3], Timothée Delubac[72], Aleksandar M. Diamond-Stanic[43], John Donor[17], Juan José Downes[73], Niv Drory[74], Hélion du Mas des Bourboux[13], Christopher J. Duckworth[20], Tom Dwelly[55], Jamie Dyer[22], Garrett Ebelke[10], Arthur Davis Eigenbrot[30], Daniel J. Eisenstein[75], Yvonne P. Elsworth[76], Eric Emsellem[77,78], Michael Eracleous[19,44], Ghazaleh Erfanianfar[55], Stephanie Escoffier[64], Xiaohui Fan[28], Emma Fernández Alvar[4], J. G. Fernandez-Trincado[58], Rafael Fernando Cirolini[62], Diane Feuillet[79], Alexis Finoguenov[55], Scott W. Fleming[59], Andreu Font-Ribera[80], Gordon Freischlad[33], Peter Frinchaboy[17], Hai Fu[81], Yilen Gómez Maqueo Chew[4], Lluís Galbany[9], Ana E. García Pérez[2,3], R. Garcia-Dias[2,3], D. A. García-Hernández[2,3], Luis Alberto Garma Oehmichen[4], Patrick Gaulme[33], Joseph Gelfand[36], Héctor Gil-Marín[82,83], Bruce A. Gillespie[33], Daniel Goddard[31], Jonay I. González Hernández[2,3], Violeta Gonzalez-Perez[31], Kathleen Grabowski[33], Paul J. Green[75], Catherine J. Grier[19,44], Alain Gueguen[55], Hong Guo[84], Julien Guy[71], Alex Hagen[19], Patrick Hall[85], Paul Harding[86], Sten Hasselquist[34], Suzanne Hawley[8], Christian R. Hayes[10], Fred Hearty[44], Saskia Hekker[87], Jesus Hernandez[116], Hector Hernandez Toledo[4], David W. Hogg[36], Kelly Holley-Bockelmann[32], Jon A. Holtzman[34], Jiamin Hou[55,88], Bau-Ching Hsieh[89], Jason A. S. Hunt[42], Timothy A. Hutchinson[22], Ho Seong Hwang[54], Camilo Eduardo Jimenez Angel[2,3], Jennifer A. Johnson[90,91], Amy Jones[92], Henrik Jönsson[2,3], Eric Jullo[37], Fahim Sakil Khan[43], Karen Kinemuchi[33], David Kirkby[1], Charles C. Kirkpatrick IV[93], Francisco-Shu Kitaura[2,3], Gillian R. Knapp[94], Jean-Paul Kneib[72], Juna A. Kollmeier[23], Ivan Lacerna[40,95,96], Richard R. Lane[40,95], Dustin Lang[42], David R. Law[59], Jean-Marc Le Goff[13], Young-Bae Lee[53], Hongyu Li[97], Cheng Li[98], Jianhui Lian[31], Yu Liang[98], Marcos Lima[62,99], Lihwai Lin (林俐暉)[89], Dan Long[33], Sara Lucatello[100], Britt Lundgren[101], J. Ted Mackereth[102], Chelsea L. MacLeod[75], Suvrath Mahadevan[44], Marcio Antonio Geimba Maia[62,63], Steven Majewski[10], Arturo Manchado[2,3], Claudia Maraston[31], Vivek Mariappan[22], Rui Marques-Chaves[2,3], Thomas Masseron[2,3], Karen L. Masters (何凱論)[31,134,130], Richard M. McDermid[103], Ian D. McGreer[28], Matthew Melendez[17], Sofia Meneses-Goytia[31], Andrea Merloni[55], Michael R. Merrifield[11], Szabolcs Meszaros[104,137], Andres Meza[105,106], Ivan Minchev[7], Dante Minniti[40,105,107], Eva-Maria Mueller[31], Francisco Muller-Sanchez[60], Demitri Muna[91], Ricardo R. Muñoz[108], Adam D. Myers[109], Preethi Nair[110], Kirpal Nandra[55], Melissa Ness[79], Jeffrey A. Newman[9], Robert C. Nichol[31], David L. Nidever[38], Christian Nitschelm[12], Pasquier Noterdaeme[111], Julia O'Connell[17], Ryan James Oelkers[32], Audrey Oravetz[33], Daniel Oravetz[33], Erik Aquino Ortíz[4], Yeisson Osorio[2,3], Zach Pace[30], Nelson Padilla[95], Nathalie Palanque-Delabrouille[13], Pedro Alonso Palicio[2,3], Hsi-An Pan[89], Kaike Pan[33], Taniya Parikh[31], Isabelle Pâris[37], Changbom Park[54], Sebastien Peirani[111], Marcos Pellejero-Ibanez[2,3], Samantha Penny[31], Will J. Percival[31], Ismael Perez-Fournon[2,3], Patrick Petitjean[111], Matthew M. Pieri[37], Marc Pinsonneault[90], Alice Pisani[64], Francisco Prada[112,113], Abhishek Prakash[9,131], Anna Bárbara de Andrade Queiroz[61,62], M. Jordan Raddick[18], Anand Raichoor[72], Sandro Barboza Rembold[62,66], Hannah Richstein[17], Rogemar A. Riffel[62,66], Rogério Riffel[61,62], Hans-Walter Rix[79], Annie C. Robin[114], Sergio Rodríguez Torres[115], Carlos Román-Zúñiga[116], Ashley J. Ross[91], Graziano Rossi[53], John Ruan[8], Rossana Ruggeri[31], Jose Ruiz[43], Mara Salvato[55], Ariel G. Sánchez[55], Sebastián F. Sánchez[4], Jorge Sanchez Almeida[2,3], José R. Sánchez-Gallego[8], Felipe Antonio Santana Rojas[108], Basílio Xavier Santiago[61,62], Ricardo P. Schiavon[102], Jaderson S. Schimoia[61,62], Edward Schlafly[15], David Schlegel[15], Donald P. Schneider[19,44], William J. Schuster[116], Axel Schwope[7], Hee-Jong Seo[117], Aldo Serenelli[118,132], Shiyin Shen[84], Yue Shen[119,120], Matthew Shetrone[74], Michael Shull[60], Víctor Silva Aguirre[121], Joshua D. Simon[23], Mike Skrutskie[10],

Anže Slosar[122], Rebecca Smethurst[11], Verne Smith[38], Jennifer Sobeck[8], Garrett Somers[32], Barbara J. Souter[18], Diogo Souto[63], Ashley Spindler[123], David V. Stark[124], Keivan Stassun[32], Matthias Steinmetz[7], Dennis Stello[121,125,126], Thaisa Storchi-Bergmann[61,62], Alina Streblyanska[2,3], Guy S. Stringfellow[60], Genaro Suárez[116], Jing Sun[17], Laszlo Szigeti[104], Manuchehr Taghizadeh-Popp[18], Michael S. Talbot[22], Baitian Tang[58], Charling Tao[64,98], Jamie Tayar[90], Mita Tembe[10], Johanna Teske[23], Aniruddha R. Thakar[18], Daniel Thomas[31], Patricia Tissera[105], Rita Tojeiro[20], Christy Tremonti[30], Nicholas W. Troup[10], Meg Urry[6], O. Valenzuela[47,136], Remco van den Bosch[79], Jaime Vargas-González[68], Mariana Vargas-Magaña[69], Jose Alberto Vazquez[122], Sandro Villanova[58], Nicole Vogt[34], David Wake[101,123], Yuting Wang[97], Benjamin Alan Weaver[38], Anne-Marie Weijmans[20], David H. Weinberg[90,91], Kyle B. Westfall[27], David G. Whelan[127], Eric Wilcots[30], Vivienne Wild[20], Rob A. Williams[102], John Wilson[10], W. M. Wood-Vasey[9], Dominika Wylezalek[52], Ting Xiao (肖婷)[84], Renbin Yan[128], Meng Yang[20], Jason E. Ybarra[129], Christophe Yèche[13], Nadia Zakamska[18], Olga Zamora[2,3], Pauline Zarrouk[13], Gail Zasowski[22,59], Kai Zhang[128], Cheng Zhao[98], Gong-Bo Zhao[31,97], Zheng Zheng[22], Zheng Zheng[97], Zhi-Min Zhou[97], Guangtun Zhu[52,135], Joel C. Zinn[90], and Hu Zou[97]

[1] Department of Physics and Astronomy, University of California, Irvine, Irvine, CA 92697, USA
[2] Instituto de Astrofísica de Canarias, E-38205 La Laguna, Tenerife, Spain
[3] Departamento de Astrofísica, Universidad de La Laguna (ULL), E-38206 La Laguna, Tenerife, Spain
[4] Instituto de Astronomía, Universidad Nacional Autónoma de México, A.P. 70-264, 04510, México, D.F., México
[5] Instituto de Investigaciòn Multidisciplinario en Ciencia y Tecnologìa, Universidad de La Serena, Benavente 980, La Serena, Chile
[6] Yale Center for Astronomy and Astrophysics, Yale University, New Haven, CT, 06520, USA
[7] Leibniz-Institut für Astrophysik Potsdam (AIP), An der Sternwarte 16, D-14482 Potsdam, Germany
[8] Department of Astronomy, Box 351580, University of Washington, Seattle, WA 98195, USA
[9] PITT PACC, Department of Physics and Astronomy, University of Pittsburgh, Pittsburgh, PA 15260, USA
[10] Department of Astronomy, University of Virginia, 530 McCormick Road, Charlottesville, VA 22904-4325, USA
[11] School of Physics & Astronomy, University of Nottingham, Nottingham, NG7 2RD, UK
[12] Unidad de Astronomía, Fac. Cs. Básicas, Universidad de Antofagasta, Avda. U. de Antofagasta 02800, Antofagasta, Chile
[13] CEA/Irfu, Universit e Paris-Saclay, F-91191 Gif-sur-Yvette, France
[14] APC, University of Paris Diderot, CNRS/IN2P3, CEA/IRFU, Observatoire de Paris, Sorbonne Paris Cite, France
[15] Lawrence Berkeley National Laboratory, 1 Cyclotron Road, Berkeley, CA 94720, USA
[16] LPNHE, Sorbonne Université, CNRS-IN2P3, 4 Place Jussieu, F-75005 Paris, France
[17] Department of Physics and Astronomy, Texas Christian University, Fort Worth, TX 76129, USA
[18] Department of Physics and Astronomy, Johns Hopkins University, 3400 N. Charles St., Baltimore, MD 21218, USA
[19] Institute for Gravitation and the Cosmos, The Pennsylvania State University, University Park, PA 16802, USA
[20] School of Physics and Astronomy, University of St Andrews, North Haugh, St Andrews, KY16 9SS, UK
[21] Humboldt-Universität zu Berlin, Institut für Physik, Newtonstrasse 15, D-12589, Berlin, Germany
[22] Department of Physics and Astronomy, University of Utah, 115 S. 1400 E., Salt Lake City, UT 84112, USA
[23] The Observatories of the Carnegie Institution for Science, 813 Santa Barbara St., Pasadena, CA 91101, USA
[24] Department of Physics and JINA Center for the Evolution of the Elements, University of Notre Dame, Notre Dame, IN 46556, USA
[25] Cavendish Laboratory, University of Cambridge, 19 J. J. Thomson Avenue, Cambridge CB3 0HE, UK
[26] Kavli Institute for Cosmology, University of Cambridge, Madingley Road, Cambridge CB3 0HA, UK
[27] University of California Observatories, University of California, Santa Cruz, Santa Cruz, CA 95064, USA
[28] Steward Observatory, The University of Arizona, 933 North Cherry Avenue, Tucson, AZ 85721–0065, USA
[29] Department of Physics and Astronomy, University of Pennsylvania, Philadelphia, PA 19104, USA
[30] Department of Astronomy, University of Wisconsin-Madison, 475 N. Charter St., Madison, WI 53726, USA
[31] Institute of Cosmology & Gravitation, University of Portsmouth, Dennis Sciama Building, Portsmouth, PO1 3FX, UK
[32] Vanderbilt University, Department of Physics & Astronomy, 6301 Stevenson Center Ln., Nashville, TN 37235, USA
[33] Apache Point Observatory, P.O. Box 59, Sunspot, NM 88349, USA
[34] Department of Astronomy, New Mexico State University, Box 30001, MSC 4500, Las Cruces NM 88003, USA
[35] Sternberg Astronomical Institute, Moscow State University, Moscow, Russia
[36] Center for Cosmology and Particle Physics, Department of Physics, New York University, 726 Broadway, Room 1005, New York, NY 10003, USA
[37] Aix-Marseille Université, CNRS, LAM, Laboratoire d'Astrophysique de Marseille, Marseille, France
[38] National Optical Astronomy Observatory, 950 North Cherry Avenue, Tucson, AZ 85719, USA
[39] Departamento de Fìsica y Astronomìa, Universidad de Valparaìriso, Av. Gran Breta na 1111, Playa Ancha, Casilla 5030, Valparaiso, Chile
[40] Instituto Milenio de Astrofísica, Av. Vicuña Mackenna 4860, Macul, Santiago, Chile
[41] Department of Astronomy and Astrophysics, University of Toronto, 50 St. George Street, Toronto, ON, M5S 3H4, Canada
[42] Dunlap Institute for Astronomy and Astrophysics, University of Toronto, 50 St. George Street, Toronto, Ontario M5S 3H4, Canada
[43] Department of Physics and Astronomy, Bates College, 44 Campus Avenue, Lewiston, ME 04240, USA
[44] Department of Astronomy and Astrophysics, Eberly College of Science, The Pennsylvania State University, 525 Davey Laboratory, University Park, PA 16802, USA
[45] Department of Physics, The Pennsylvania State University, University Park, PA 16802, USA
[46] Center for Astrophysics and Space Science, University of California San Diego, La Jolla, CA 92093, USA
[47] Instituto de Astronomía, Universidad Nacional Autónoma de México, A.P. 70-264, 04510, México, D.F., México
[48] Sub-department of Astrophysics, Department of Physics, University of Oxford, Denys Wilkinson Building, Keble Road, Oxford OX1 3RH, UK
[49] School of Physics & Astronomy, Monash University, Wellington Road, Clayton, Victoria 3800, Australia
[50] Instituto de Radioastronomía y Astrofísica, Universidad Nacional Autónoma de México, Campus Morelia, A.P. 3-72, C.P. 58089 Michoacán, México
[51] NYU Abu Dhabi, P.O. Box 129188, Abu Dhabi, UAE
[52] Center for Astrophysical Sciences, Department of Physics and Astronomy, Johns Hopkins University, 3400 North Charles Street, Baltimore, MD 21218, USA; spokesperson@sdss.org
[53] Department of Astronomy and Space Science, Sejong University, Seoul 143-747, People's Republic of Korea
[54] Korea Institute for Advanced Study, 85 Hoegiro, Dongdaemun-gu, Seoul 02455, People's Republic of Korea
[55] Max-Planck-Institut für extraterrestrische Physik, Gießenbachstr. 1, D-85748 Garching, Germany
[56] CNRS, IRAP, 9 Av.Colonel Roche, BP 44346, F-31028 Toulouse cedex 4, France
[57] Université de Toulouse, UPS-OMP, IRAP, Toulouse, France
[58] Departamento de Astronomia, Casilla 160-C, Universidad de Concepcion, Concepcion, Chile

[59] Space Telescope Science Institute, 3700 San Martin Drive, Baltimore, MD 21218, USA
[60] Center for Astrophysics and Space Astronomy, Department of Astrophysical and Planetary Sciences, University of Colorado, 389 UCB, Boulder, CO 80309-0389, USA
[61] Instituto de Física, Universidade Federal do Rio Grande do Sul, Campus do Vale, Porto Alegre, RS, 91501-970, Brasil,
[62] Laboratório Interinstitucional de e-Astronomia, 77 Rua General José Cristino, Rio de Janeiro, 20921-400, Brasil
[63] Observatório Nacional, Rio de Janeiro, Brasil
[64] Aix-Marseille Université, CNRS/IN2P3, CPPM, Marseille, France
[65] Department of Physics and Astronomy, Western Washington University, 516 High Street, Bellingham, WA 98225, USA
[66] Departamento de Física, CCNE, Universidade Federal de Santa Maria, 97105-900, Santa Maria, RS, Brazil
[67] Centro Multidisciplinario de Ciencia y Tecnologia, Universidad de La Serena, Cisternas 1200, La Serena, Chile
[68] Departamento de Física, Facultad de Ciencias, Universidad de La Serena, Cisternas 1200, La Serena, Chile
[69] Instituto de Física, Universidad Nacional Autónoma de México, Apdo. Postal 20-364, México
[70] Department of Physics, Geology, and Engineering Tech, Northern Kentucky University, Highland Heights, KY 41099, USA
[71] LPNHE, CNRS/IN2P3, Université Pierre et Marie Curie Paris 6, Université Denis Diderot Paris, 4 place Jussieu, F-75252 Paris CEDEX, France
[72] Institute of Physics, Laboratory of Astrophysics, Ecole Polytechnique Fédérale de Lausanne (EPFL), Observatoire de Sauverny, 1290 Versoix, Switzerland
[73] Centro de Investigaciones de Astronomía, AP 264, Mérida 5101-A, Venezuela
[74] McDonald Observatory, The University of Texas at Austin, 1 University Station, Austin, TX 78712, USA
[75] Harvard-Smithsonian Center for Astrophysics, 60 Garden St., Cambridge, MA 02138, USA
[76] School of Physics and Astronomy, University of Birmingham, Edgbaston, Birmingham B15 2TT, UK
[77] European Southern Observatory, Karl-Schwarzschild-Str. 2, D-85748 Garching, Germany
[78] Université Lyon 1, Obs. de Lyon, CRAL, 9 avenue Charles André, F-69230 Saint-Genis Laval, France
[79] Max-Planck-Institut für Astronomie, Königstuhl 17, D-69117 Heidelberg, Germany
[80] Department of Physics & Astronomy, University College London, Gower Street, London, WC1E 6BT, UK
[81] Department of Physics & Astronomy, University of Iowa, Iowa City, IA 52245, USA
[82] Sorbonne Universités, Institut Lagrange de Paris (ILP), 98 bis Boulevard Arago, F-75014 Paris, France
[83] Laboratoire de Physique Nucléaire et de Hautes Energies, Université Pierre et Marie Curie, 4 Place Jussieu, F-75005 Paris, France
[84] Shanghai Astronomical Observatory, Chinese Academy of Science, 80 Nandan Road, Shanghai 200030, People's Republic of China
[85] Department of Physics and Astronomy, York University, 4700 Keele St., Toronto, ON, M3J 1P3, Canada
[86] Department of Astronomy, Case Western Reserve University, Cleveland, OH 44106, USA
[87] Max Planck Institute for Solar System Research, Justus- von-Liebig-Weg 3, D-37077 Goettingen, Germany
[88] Universitäts-Sternwarte München, Ludwig-Maximilians-Universität Munchen, Scheinerstrasse 1, D-81679 München, Germany
[89] Academia Sinica Institute of Astronomy and Astrophysics, P.O. Box 23-141, Taipei 10617, Taiwan
[90] Department of Astronomy, Ohio State University, 140 W. 18th Ave., Columbus, OH 43210, USA
[91] Center for Cosmology and AstroParticle Physics, The Ohio State University, 191 W. Woodruff Ave., Columbus, OH 43210, USA
[92] Max-Planck-Institut für Astrophysik, Karl-Schwarzschild-Str. 1, D-85748 Garching, Germany
[93] Department of Physics, University of Helsinki, Gustaf Hällströmin katu 2a, FI-00014 Helsinki, Finland
[94] Department of Astrophysical Sciences, Princeton University, Princeton, NJ 08544, USA
[95] Instituto de Astrofísica, Pontificia Universidad Católica de Chile, Av. Vicuna Mackenna 4860, 782-0436 Macul, Santiago, Chile
[96] Astrophysical Research Consortium, Physics/Astronomy Building, Rm C319, 3910 15th Avenue NE, Seattle, WA 98195, USA
[97] National Astronomical Observatories, Chinese Academy of Sciences, 20A Datun Road, Chaoyang District, Beijing 100012, People's Republic of China
[98] Tsinghua Center for Astrophysics & Department of Physics, Tsinghua University, Beijing 100084, People's Republic of China
[99] Departamento de Física Matemática, Instituto de Física, Universidade de São Paulo, CP 66318, CEP 05314-970, São Paulo, SP, Brazil
[100] Astronomical Observatory of Padova, National Institute of Astrophysics, Vicolo Osservatorio 5, I-35122—Padova, Italy
[101] Department of Physics, University of North Carolina Asheville, One University Heights, Asheville, NC 28804, USA
[102] Astrophysics Research Institute, Liverpool John Moores University, IC2, Liverpool Science Park, 146 Brownlow Hill, Liverpool L3 5RF, UK
[103] Department of Physics and Astronomy, Macquarie University, Sydney NSW 2109, Australia
[104] ELTE Eötvös Loránd University, Gothard Astrophysical Observatory, Szombathely, Hungary
[105] Departamento de Física, Facultad de Ciencias Exactas, Universidad Andres Bello, Av. Fernandez Concha 700, Las Condes, Santiago, Chile
[106] Facultad de Ingeniería, Universidad Autónoma de Chile, Pedro de Valdivia 425, Santiago, Chile
[107] Vatican Observatory, V00120 Vatican City State, Italy
[108] Universidad de Chile, Av. Libertador Bernardo O'Higgins 1058, Santiago de Chile, Chile
[109] Department of Physics and Astronomy, University of Wyoming, Laramie, WY 82071, USA
[110] The University of Alabama, Tuscaloosa, AL 35487, USA
[111] Institut d'Astropysique de Paris, UMR 7095, CNRS—UPMC, 98bis bd Arago, F-75014 Paris, France
[112] Instituto de Física Teórica (IFT) UAM/CSIC, Universidad Autónoma de Madrid, Cantoblanco, E-28049 Madrid, Spain
[113] Instituto de Astrofisica de Andalucia (IAA-CSIC), Glorieta de la Astronomia s/n, E-18008, Granada, Spain
[114] Institut UTINAM, CNRS UMR6213, Univ. Bourgogne Franche-Comté, OSU THETA Franche-Comté-Bourgogne, Observatoire de Besançon, BP 1615, F-25010 Besançon Cedex, France
[115] Departamento de Física Teórica M8, Universidad Autonóma de Madrid (UAM), Cantoblanco, E-28049, Madrid, Spain
[116] Instituto de Astronomía, Universidad Nacional Autónoma de México, Unidad Académica en Ensenada, Ensenada BC 22860, México
[117] Department of Physics and Astronomy, Ohio University, Clippinger Labs, Athens, OH 45701, USA
[118] Institute of Space Sciences (CSIC-IEEC), Carrer de Can Magrans S/N, Campus UAB, Barcelona, E-08193, Spain
[119] Department of Astronomy, University of Illinois, 1002 W. Green Street, Urbana, IL 61801, USA
[120] National Center for Supercomputing Applications, 1205 West Clark St., Urbana, IL 61801, USA
[121] Stellar Astrophysics Centre, Department of Physics and Astronomy, Aarhus University, Ny Munkegade 120, DK-8000 Aarhus C, Denmark
[122] Brookhaven National Laboratory, Upton, NY 11973, USA
[123] Department of Physical Sciences, The Open University, Milton Keynes, MK7 6AA, UK
[124] Kavli Institute for the Physics and Mathematics of the Universe, Todai Institutes for Advanced Study, The University of Tokyo, Kashiwa 277-8583, Japan
[125] Sydney Institute for Astronomy, School of Physics, University of Sydney, NSW 2006, Australia
[126] School of Physics, University of New South Wales, NSW 2052, Australia
[127] Department of Physics, Austin College, Sherman, TX 75090, USA
[128] Department of Physics and Astronomy, University of Kentucky, 505 Rose St., Lexington, KY, 40506-0055, USA
[129] Department of Physics, Bridgewater College, 402 E. College St., Bridgewater, VA 22812 USA
[130] Haverford College, Department of Physics and Astronomy, 370 Lancaster Avenue, Haverford, Pennsylvania 19041, USA

[131] Infrared Processing and Analysis Center (IPAC), California Institute of Technology, 1200 E California Blvd, Pasadena, CA 91125, USA
[132] Institut d'Estudis Espacials de Catalunya (IEEC), C/Gran Capita, 2-4, E-08034, Barcelona, Spain
Received 2017 July 28; revised 2017 November 28; accepted 2017 November 28; published 2018 April 19

Abstract

The fourth generation of the Sloan Digital Sky Survey (SDSS-IV) has been in operation since 2014 July. This paper describes the second data release from this phase, and the 14th from SDSS overall (making this Data Release Fourteen or DR14). This release makes the data taken by SDSS-IV in its first two years of operation (2014–2016 July) public. Like all previous SDSS releases, DR14 is cumulative, including the most recent reductions and calibrations of all data taken by SDSS since the first phase began operations in 2000. New in DR14 is the first public release of data from the extended Baryon Oscillation Spectroscopic Survey; the first data from the second phase of the Apache Point Observatory (APO) Galactic Evolution Experiment (APOGEE-2), including stellar parameter estimates from an innovative data-driven machine-learning algorithm known as "The Cannon"; and almost twice as many data cubes from the Mapping Nearby Galaxies at APO (MaNGA) survey as were in the previous release ($N = 2812$ in total). This paper describes the location and format of the publicly available data from the SDSS-IV surveys. We provide references to the important technical papers describing how these data have been taken (both targeting and observation details) and processed for scientific use. The SDSS web site (www.sdss.org) has been updated for this release and provides links to data downloads, as well as tutorials and examples of data use. SDSS-IV is planning to continue to collect astronomical data until 2020 and will be followed by SDSS-V.

Key words: atlases – catalogs – surveys

1. Introduction

It is now 16 years since the first data release from the Sloan Digital Sky Survey (SDSS; York et al. 2000). This Early Data Release, or EDR, occurred in 2001 June (Stoughton et al. 2002). Since this time, annual data releases from SDSS have become part of the landscape of astronomy, populating databases used by thousands of astronomers worldwide (Raddick et al. 2014a, 2014b), and making the SDSS's 2.5 m Sloan Foundation Telescope (Gunn et al. 2006) one of the most productive observatories in the world (Madrid & Macchetto 2009). This paper describes the 14th public data release from SDSS, or DR14, released on 2017 July 31.

The SDSS has completed three phases and is currently in its fourth phase. SDSS-I and -II conducted a Legacy survey of galaxies and quasars (York et al. 2000), the SDSS-II Supernova Survey (Frieman et al. 2008; Sako et al. 2014), and conducted observations of stars for the Sloan Extension for Galactic Understanding and Exploration 1 (SEGUE-1; Yanny et al. 2009). These surveys made use of the SDSS imaging camera (Gunn et al. 1998) and 640 fiber optical spectrograph (Smee et al. 2013). SDSS-III continued observations of stars with SEGUE-2 and conducted two new surveys with new instrumentation (Eisenstein et al. 2011).

The Baryon Oscillation Spectroscopic Survey (BOSS; Dawson et al. 2013) upgraded the optical spectrograph to 1000 fibers (named the BOSS spectrograph; Smee et al. 2013) to conduct a large-volume cosmological redshift survey which built on the work of both SDSS-II (York et al. 2000) and 2dFGRS (Colless et al. 2003). At the same time, the Apache Point Observatory Galactic Evolution Experiment 1 (APOGEE-1; Majewski et al. 2017) employed a high-resolution near-infrared spectrograph to observe stars in the Milky Way. All of these observations were conducted at APO, and data were publicly released in DR12 (Alam et al. 2015).

This paper contains new data and data reductions produced by SDSS-IV (Blanton et al. 2017). SDSS-IV began observations in 2014 July and consists of three programs.

1. The extended Baryon Oscillation Spectroscopic Survey (eBOSS; Dawson et al. 2016) is surveying galaxies and quasars at redshifts $z \sim 0.6$–3.5 for large-scale structure. eBOSS covers a wider class of galaxies than BOSS at higher effective redshifts. In particular, the size and depth of the quasar sample is a huge leap forward over previous surveys. eBOSS will also observe emission-line galaxies, extending the WiggleZ survey (Blake et al. 2011) in the southern sky to a larger sample of galaxies at higher redshifts. Following from eBOSS, the TAIPAN survey (da Cunha et al. 2017) will soon provide a low-redshift complement in the southern hemisphere. All of these surveys will be eclipsed by forthcoming experiments including DESI (Aghamousa et al. 2016a, 2016b), Euclid (Laureijs et al. 2011), and 4MOST (de Jong et al. 2014), which will use new instrumentation to obtain galaxy surveys an order of magnitude larger than ongoing surveys. Two major subprograms are being conducted concurrently with eBOSS:
   (a) The SPectroscopic IDentification of ERosita Sources (SPIDERS) investigates the nature of X-ray-emitting sources, including active galactic nuclei (AGNs) and galaxy clusters. This contains the largest systematic spectroscopic follow-up sample of X-ray-selected clusters (for details, see Section 4), reaching into a regime where meaningful dynamical estimates of cluster properties are possible for hundreds of massive systems. It contains a highly complete sample of the most luminous X-ray-selected AGNs, which will only be superseded by the spectroscopic follow-up

[133] Alfred P. Sloan Fellow.
[134] SDSS-IV Spokesperson.
[135] Hubble Fellow.
[136] CONACYT Research Fellow.
[137] Premium Postdoctoral Fellow of the Hungarian Academy of Sciences.

programs of the eROSITA survey (mainly via SDSS-V and 4MOST)

(b) The Time Domain Spectroscopic Survey (TDSS; Morganson et al. 2015) is exploring the physical nature of time-variable sources through spectroscopy. The main TDSS program of optical follow-up of variables from Pan-STARRS1 imaging is the first large—by order(s) of magnitude—program of optical spectroscopy of photometrically variable objects, selected without a priori restriction based on specific photometric colors or light-curve character. About 20% of TDSS targets involve repeat spectroscopy of select classes of known objects with earlier epochs of spectroscopy, e.g., searching for variability among known broad absorption line (BAL) quasars, and building and expanding on earlier such programs (e.g., Filiz Ak et al. 2014); a comprehensive description of the latter such repeat spectroscopy programs of the TDSS may be found in MacLeod et al. (2017).

2. Mapping Nearby Galaxies at APO (MaNGA; Bundy et al. 2015) is using integral field spectroscopy (IFS) to study 10,000 nearby galaxies. MaNGA builds on a number of successful IFS surveys (e.g., ATLAS-3D, Cappellari et al. 2011; DiskMass, Bershady et al. 2010; and CALIFA, Sánchez et al. 2012), surveying a significantly larger and more diverse samples of galaxies over a broader spectral range at higher spectral resolution. It has finer spatial sampling and a final sample size three times that of the similar SAMI survey (Bryant et al. 2015), and in this release becomes the largest set of public IFS observations available.
3. APOGEE/APOGEE-2 perform a large-scale and systematic investigation of the entire Milky Way Galaxy with near-infrared, high-resolution, and multiplexed instrumentation. For APOGEE-2, observations are being carried out at both northern and southern hemisphere locations: the 2.5 m Sloan Foundation Telescope of the Apache Point Observatory (APOGEE-2N; which started Q3 2014) and the 2.5 m du Pont Telescope of the Las Campanas Observatory (APOGEE-2S; from Q2 2017). APOGEE/APOGEE-2 is the only large-scale (>1,000,000 spectra for >450,000 objects) near-IR spectroscopic survey of stars, ensuring it has a unique view of all parts of our Galaxy, unhampered by interstellar obscuration in the Galactic plane. Most stellar surveys of equivalent scale—including those that have concluded (e.g., RAVE, SEGUE-1 and −2, and *ARGOS*; Steinmetz et al. 2006, Yanny et al. 2009, Rockosi et al. 2009, Freeman et al. 2013), are currently underway (e.g., LAMOST, *Gaia*-ESO, GALAH, and *Gaia*; Cui et al. 2012, Gilmore et al. 2012, Zucker et al. 2012, Perryman et al. 2001), or are anticipated in the future (e.g., WEAVE, 4MOST, and MOONS; Dalton et al. 2014, de Jong et al. 2014, Cirasuolo et al. 2014)—have been or will be performed in the optical and/or with largely medium spectral resolution (however, we note plans for high-resolution modes for some of these). All of these projects provide complementary data in the form of different wavelength or spatial regimes providing essential contributions to the ongoing census of the Milky Way's stars.

SDSS-IV has had one previous data release (DR13; Albareti & Allende Prieto et al. 2017; for a "behind the scenes" view of how this is done, see Weijmans et al. 2016), which contained the first year of MaNGA data, new calibrations of the SDSS imaging data set, and new processing of APOGEE-1 and BOSS data (along with a small amount of BOSS-related data taken during SDSS-IV).

Table 1
Reduced Spectroscopic Data in DR14

Target Category	# DR13	# DR13+14
eBOSS		
LRG samples	32,968	138,777
ELG Pilot Survey	14,459	35,094
Main QSO Sample	33,928	188,277
Variability-selected QSOs	22,756	87,270
Other QSO samples	24,840	43,502
TDSS Targets	17,927	57,675
SPIDERS Targets	3133	16,394
Standard Stars/White Dwarfs	53,584	63,880
APOGEE-2		
All Stars	164,562	26,3444
NMSU 1 m stars	894	1018
Telluric stars	17,293	27,127
APOGEE-N Commissioning stars	11,917	12,194
MaNGA Cubes	1390	2812
MaNGA main galaxy sample:		
`PRIMARY_v1_2`	600	1278
`SECONDARY_v1_2`	473	947
`COLOR-ENHANCED_v1_2`	216	447
MaNGA ancillary targets[a]	31	121

Note.
[a] Many MaNGA ancillary targets were also observed as part of the main galaxy sample, and are counted twice in this table; some ancillary targets are not galaxies.

DR14 contains new reductions and new data for all programs, roughly covering the first two years of SDSS-IV operations. This release contains the first public release of data from eBOSS and APOGEE-2, and almost doubles the number of data cubes publicly available from MaNGA.

The full scope of the data release is described in Section 2, and information on data distribution is given in Section 3. Each of the subsurveys is described in its own section, with eBOSS (including SPIDERS and TDSS) in Section 4, APOGEE-2 in Section 5, and MaNGA in Section 6. We discuss future plans for SDSS-IV and beyond in Section 7.

2. Scope of Data Release 14

As has been the case for all public SDSS data releases, DR14 is cumulative, and includes re-releases of all previously released data processed through the most current data reduction pipelines (DRPs). In some cases, this pipeline has not changed for many DRs (see summary below). New data released in DR14 were taken by the Sloan Foundation 2.5 m telescope between 2014 August 23 (MJD = 56893)[138] and 2016 July 10 (MJD = 57580). The full scope of the release is summarized in Table 1.

We discuss the data released by each of the main surveys in detail below, but briefly, DR14 includes

1. Data from 496 new eBOSS plates covering ∼2480 square degrees observed from 2014 September to 2016 May. We

[138] This is the date for eBOSS; for APOGEE and MaNGA, it was 2015 July.

Table 2
Value Added Catalogs New to DR14

Description	Reference(s)
APOGEE:	
DR14 APOGEE red-clump catalog	Bovy et al. (2014)
DR14 APOGEE-TGAS Catalog	F. Anders et al. (2018, in preparation)
APOGEE DR14 Distance Estimations from Four Groups	
BPG (Bayesian Method)	Santiago et al. (2016), Queiroz et al. (2018)
NAOC (Bayesian Method)	Wang et al. (2016)
NICE (Isochrone-matching Technique)	Schultheis et al. (2014)
NMSU (Bayesian Method)	J. Holtzman et al. (2018, in preparation)
eBOSS/TDSS/SPIDERS:	
Redshift Measurement and Spectral Classification Catalog with Redmonster	Hutchinson et al. (2016)
eBOSS: Emission Line Galaxy (ELG) Target Catalog	Raichoor et al. (2017)
FIREFLY Stellar Population Models of SDSS-I–SDSS-III and eBOSS galaxy spectra	Comparat et al. (2017)
The SDSS-DR14 Quasar Catalog	Pâris et al. (2017b)
Composite Spectra of BOSS Quasars Binned on Spectroscopic Parameters from DR12Q	Jensen et al. (2016)
SPIDERS X-ray galaxy cluster catalog for DR14	Clerc et al. (2016)
The Brightest Cluster Galaxy properties of SPIDERS X-ray galaxy clusters	G. Erfanianfar et al. (2018, in preparation)
Multiwavelength properties of RASS AGN	A. Merloni et al. (2018, in preparation)
Multiwavelength properties of XMMSL AGN	A. Del Moro et al. (2018, in preparation)
MaNGA:	
MaNGA Pipe3D: Spatially resolved and integrated properties of galaxies	Sánchez et al. (2016a, 2016b, 2017a)
MaNGA FIREFLY Stellar Populations	Goddard et al. (2017)

also include data from a transitional project between BOSS and eBOSS called the Sloan Extended Quasar, ELG, and Luminous Red Galaxy (LRG) Survey (SEQUELS), designed to test target-selection algorithms for eBOSS. The complete SEQUELS data set was previously released in DR13; however, DR14 is the first release for eBOSS. The eBOSS data contain mainly LRG and quasar spectra, as well as targets from TDSS and SPIDERS. Twenty-three new eBOSS Emission Line Galaxy (ELG) plates are included in DR14 to test final target-selection algorithms. The full ELG survey started collecting spectra in 2016 September and will be part of a future data release. We include in DR14 the first part of the ELG target catalog (see Table 2) described in Raichoor et al. (2017). Other eBOSS value added catalogs (VACs) are also released, namely (1) the redshift measurement and spectral classification catalog using Redmonster (Hutchinson et al. 2016), (2) the quasar catalog (Pâris et al. 2017b), and (3) a set of composite spectra of quasars binned on spectroscopic parameters (Jensen et al. 2016).

2. APOGEE visit-combined spectra as well as pipeline-derived stellar atmospheric parameters and individual elemental abundances for more than 263,000 stars, sampling all major components of the Milky Way. This release includes all APOGEE-1 data from SDSS-III (2011 August–2014 July) as well as two years of APOGEE-2 data from SDSS-IV (2014 July–2016 July). APOGEE VACs include (1) an updated version of the APOGEE red-clump catalog (APOGEE-RC; Pinsonneault et al. 2018) (2) a cross-match between APOGEE and the Tycho-*Gaia* Astrometric Solution (APOGEE-TGAS; F. Anders et al. 2018, in preparation), and (3) a compilation of four different methods to estimate distances to APOGEE stars (Schultheis et al. 2014; Santiago et al. 2016; Wang et al. 2016; J. Holtzman et al. 2018, in preparation; Queiroz et al. 2018).
3. Data from 166 MaNGA plates, which result in 2812 reconstructed 3D data cubes (for 2744 unique galaxies, primarily from the main MaNGA target sample, but these data also include ancillary targets and ∼50 repeat observations). Internally, this set of galaxies has been referred to as MaNGA Product Launch-5 (MPL-5); however, the reduction pipeline is a different version from that internal release. The new data relative to what was released in DR13 were taken between 2015 August 13 (MJD = 57248) and 2016 July 10. The MaNGA release also includes two VACs, which provide spatially resolved stellar population and ionized gas properties from PIPE3D (Sánchez et al. 2016a, 2016b; see Section 6.4.1) and FIREFLY (Goddard et al. 2017; see Section 6.4.2).
4. The largest ever number of SDSS VACs produced by scientists in the collaboration—12 in total. See Table 2.
5. A re-release of the most current reduction of all data from previous versions of SDSS. In some cases, the DRP has not changed for many DRs, and so has not been re-run. The most recent imaging was released in DR13 (Albareti & Allende Prieto et al. 2017); however, only the photometric calibrations changed in that release; the astrometry is the same as in DR9 (Ahn et al. 2012) and the area released and the other aspects of the photometric reduction remain the same as that in DR8 (Aihara et al. 2011). Legacy Spectra (those observed with the SDSS spectrograph) have also not changed since DR8. There have also been no changes to SEGUE-1 or SEGUE-2 since DR9, or MARVELS since DR12 (Alam et al. 2015). For DR14, we have re-reduced BOSS spectra using the eBOSS pipeline, where flux calibration has been improved by adding new atmospheric distortion

corrections at the per-exposure level (Margala et al. 2016) and by employing an unbiased coaddition algorithm.

3. Data Distribution

The DR14 data are distributed through the same mechanisms as DR13, with the addition of a Web application to interactively interface with optical and infrared spectra. We describe our three distribution mechanisms below. These methods are also documented on the SDSS Web site (http://www.sdss.org/dr14/data_access), and tutorial examples for accessing and working with SDSS data can be found at http://www.sdss.org/dr14/tutorials.

The raw and processed imaging and spectroscopic data, as well as the VACs, are available through the Science Archive Server (SAS, data.sdss.org/sas/dr14). Data can be downloaded from the SAS directly by browsing the directory structure, and also in bulk using rsync, wget, and Globus Online (see http://www.sdss.org/dr14/data_access/bulk for more details). The data files available on the SAS all have their own data model, which describes the content of each file in detail. These data models are available at https://data.sdss.org/datamodel.

The processed imaging and optical and infrared spectra on the SAS are also available through an interactive Web application (https://dr14.sdss.org). This Web application allows the user to search for spectra based on specific parameters, e.g., plate, redshift, coordinates, or observing program. Searches can be saved through permalinks, and options are provided to download the spectra directly from the SAS, either individually or in bulk. Previous data releases back to DR8 are available through the same interface. A link is also provided to the SkyServer explore page for each object.

Finally, the DR14 data can be found on the Catalog Archive Server (CAS; Thakar 2008; Thakar et al. 2008). The CAS stores catalogs of the photometric, spectroscopic, and derived quantities; these are available through the SkyServer Web application (http://skyserver.sdss.org) for browser-based queries in synchronous mode and through CasJobs (http://skyserver.sdss.org/casjobs), which offers more advanced and extensive query options in asynchronous or batch mode, with more time-consuming queries able to run in the background (Li & Thakar 2008). The CAS is part of the SciServer (http://www.sciserver.org) collaborative science framework, which provides users access to a collection of data-driven collaborative science services, including SkyServer and CasJobs. Other services include SciDrive, a "drag-and-drop" file hosting system that allows users to share files; SkyQuery, a database system for cross-matching astronomical multiwavelength catalogs; and SciServer Compute, a system that allows users to upload analysis scripts as Jupyter notebooks (supporting Python, MatLab, and R) and run these databases in Docker containers.

In addition to the data, the data processing software used by the APOGEE-2, eBOSS, and MaNGA teams to derive their data products from the raw frames is available at http://www.sdss.org/dr14/software/products.

4. eBOSS, TDSS, and SPIDERS

eBOSS (Dawson et al. 2016) is surveying galaxies and quasars at redshifts $z \sim 0.6$–3.5 to map the large-scale structure of the universe, with the main goal to provide Baryonic Acoustic Oscillation (BAO) measurements in the uncharted redshift change spanning $0.6 < z < 2.2$. eBOSS achieves this by observing a new set of targets: high-redshift LRGs, ELGs, and quasars. The three new tracers will provide BAO distance measurements with a precision of 1% at $z = 0.7$ (LRGs), 2% at $z = 0.85$ (ELGs), and 2% at $z = 1.5$ (quasars). The Lyα forest imprinted on approximately 120,000 new quasar spectra will give eBOSS an improved BAO measurement of 1.4× over that achieved by BOSS (Delubac et al. 2015; Bautista et al. 2017). Furthermore, the clustering from eBOSS tracers will allow new measurements of redshift-space distortions, non-Gaussianity in the primordial density field, and the summed mass of neutrino species. eBOSS will provide the first percent-level distance measurements with BAO in the redshift range $0.6 < z < 3$, when cosmic expansion transitioned from deceleration to acceleration. The new redshift coverage of eBOSS obtained by targeting three classes of targets (LRGs, ELGs, and quasars) will have the statistical power to improve constraints relative to BOSS by up to a factor of 1.5 in Ω_M, a factor of three in the Dark Energy Task Force Figure of Merit (Albrecht et al. 2006), and a factor of 1.8 in the sum of the neutrino masses (Zhao et al. 2016).

We show in Figure 1 the $N(z)$ in eBOSS DR14 QSO and LRG targets compared to the final BOSS release in DR12 (Alam et al. 2015), demonstrating how eBOSS is filling in the redshift desert between $z \sim 0.8$–2.0. DR14 does not contain any significant number of ELG targets, which will be released in future DRs.

A significant number of fibers on the eBOSS plates are devoted to two additional dark-time programs. TDSS (TDSS; Morganson et al. 2015) seeks to understand the nature of celestial variables by targeting objects that vary in combined SDSS DR9 and Pan-STARRS1 data (PS1; Kaiser et al. 2002). A large number of the likely TDSS quasar targets are also targeted by the main eBOSS algorithms and therefore meet the goals of both surveys. TDSS-only targets fill ∼10 spectra per square degree. SPIDERS aims to characterize a subset of X-ray sources identified by eROSITA (extended *Roentgen* Survey with an Imaging Telescope Array; Predehl et al. 2014). However, until the first catalog of eROSITA sources is available, SPIDERS will target sources from the RASS (*Roentgen* All-Sky Survey; Voges et al. 1999) and *XMM-Newton* (*X-ray Multi-mirror Mission*; Jansen et al. 2001). SPIDERS will also obtain on average ∼10 spectra per square degree over the course of SDSS-IV, but the number of fibers per square degree on a plate is weighted toward the later years to take advantage of the new data from eROSITA.

A small fraction of eBOSS time is dedicated to an ancillary program to perform multi-object reverberation mapping for a single 7 deg^2 field. This program (SDSS-RM) aims to detect the lags between the broad-line flux and continuum flux in quasars over a broad range of redshift and luminosity with spectroscopic monitoring, which allows the measurement of the masses of these quasar black holes. Started as an ancillary program in SDSS-III, SDSS-RM continues in SDSS-IV with ∼12 epochs (each at nominal eBOSS depth) per year to extend the time baseline of the monitoring and to detect lags on multiyear timescales. The details of the SDSS-RM program can be found in Shen et al. (2015), and initial results on lag detections are reported in Shen et al. (2016) and Grier et al. (2017).

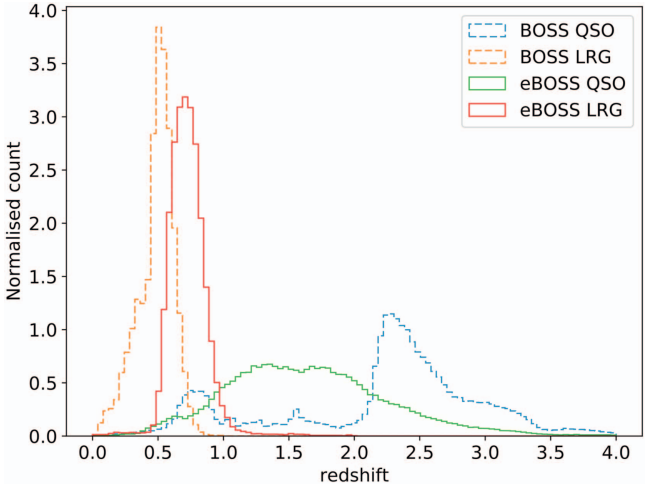

Figure 1. $N(z)$ of eBOSS DR14 QSOs and LRGs compared to DR12 BOSS, demonstrating how eBOSS is filling in the redshift desert between $z \sim 0.8$–2.0. Note that this shows only QSO and LRG targets because no significant number of ELGs has been released in DR14. To convert from normalized count to number as a function of redshift, multiply by the total numbers (given in Table 1 for the full survey) times the bin size of $dz = 0.04$.

eBOSS started in 2014 September by taking spectra of LRGs and quasars, while further development on the definition of the ELG targets sample was conducted in parallel. In 2016 May, eBOSS completed its first major cosmological sample containing LRGs and quasars from the first two years of eBOSS data and from SEQUELS (already part of the DR13 release). These data have already been used to improve the classification of galaxy spectra (Hutchinson et al. 2016), introduce new techniques to the modeling of incompleteness in galaxy clustering, and to provide measurements of clustering on BAO scales at $1 < z < 2$ for the first time (Ata et al. 2017).

4.1. Data Description

DR14 includes the data from 496 plates observed under the eBOSS program; it also includes the 126 SEQUELS plates (already released in DR13) from an ancillary program to take advantage of some of the dark time released when BOSS was completed early. The SEQUELS targets are similar to the eBOSS targets as it was a program to test the selection algorithms of eBOSS, in particular the LRG (Prakash et al. 2016) and quasar algorithms (Myers et al. 2015). The final ELG target recipe does not follow the one tested during SEQUELS. The new ELG recipe is documented in the DR14 release following the description given by Raichoor et al. (2017).

For the TDSS program, combined SDSS DR9 and Pan-STARRS1 data (PS1; Kaiser et al. 2002) are used to select variable object targets (Morganson et al. 2015; Ruan et al. 2016), while for SPIDERS, the objects are selected from a combination of X-ray and optical imaging for the SPIDERS cluster (Clerc et al. 2016) and AGN (Dwelly et al. 2017) programs.

The sky distribution of the DR14 data from eBOSS is shown in Figure 2. Table 3 summarizes the content and gives brief explanations of the targeting categories.

4.2. Retrieving eBOSS Data

All SDSS data releases are cumulative and therefore the eBOSS data also include the SEQUELS data taken in SDSS-III or SDSS-IV, reduced with the latest pipelines. eBOSS targets can be identified using the EBOSS_TARGET1 bitmask. The summary `spAll-v5_10_0.fits` data file, which includes classification information from the pipeline, is located on the SAS[139]; the data can also be queried via the `specObjAll` table on the CAS.

4.3. eBOSS/TDSS/SPIDERS VACs

We include seven VACs based on BOSS, eBOSS, TDSS, or SPIDERS data or target selection in this DR. Brief details of each are given below, and for more details we refer the reader to the relevant papers in Table 2.

4.3.1. Redshift Measurement and Spectral Classification Catalog with Redmonster

The Redmonster software[140] is a sophisticated and flexible set of Python utilities for redshift measurement, physical parameter measurement, and classification of one-dimensional astronomical spectra. A full description of the software is given in Hutchinson et al. (2016). The software approaches redshift measurement and classification as a χ^2 minimization problem by cross-correlating the observed spectrum with a theoretically motivated template within a spectral template class over a discretely sampled redshift interval. In this VAC, the software has been run on all DR14 LRG spectra. Redmonster was able to successfully measure redshifts for ∼90% of LRG spectra in DR14. This is an increase of ∼15%, in absolute terms, over `spectro1d`, and nearly matches the most optimistic estimate for the fraction of measurable redshifts as determined by visual inspections.

4.3.2. The SDSS-IV eBOSS: ELG Target Catalog

We publish the south galactic cap ELG catalog used for eBOSS (Raichoor et al. 2017). Targets were selected using photometric data from the Dark Energy Camera Legacy Survey (DECaLS; http://legacysurvey.org/). We selected roughly 240 ELG targets per square degree. The great majority of these ELGs lie in the redshift range $0.67 < z < 1.1$ (median redshift 0.85).

4.4. FIREFLY Stellar Population Models of SDSS-I–SDSS-III and eBOSS Galaxy Spectra

We determine the stellar population properties—age, metallicity, dust reddening, stellar mass, and star formation history—for all spectra classified as galaxies that were published in this release (including those from SDSS-I–SDSS-III). We perform full spectral fitting on individual spectra, making use of high spectral resolution stellar population models published in Wilkinson et al. (2017). Calculations are carried out for several choices of the model input, including three stellar initial mass functions and three input stellar libraries to the models. We study the accuracy of parameter derivation, in particular the stellar mass, as a function of the signal-to-noise ratio (S/N) of the galaxy

[139] https://data.sdss.org/sas/dr14/eboss/spectro/redux/v5_10_0/
[140] https://github.com/timahutchinson/redmonster

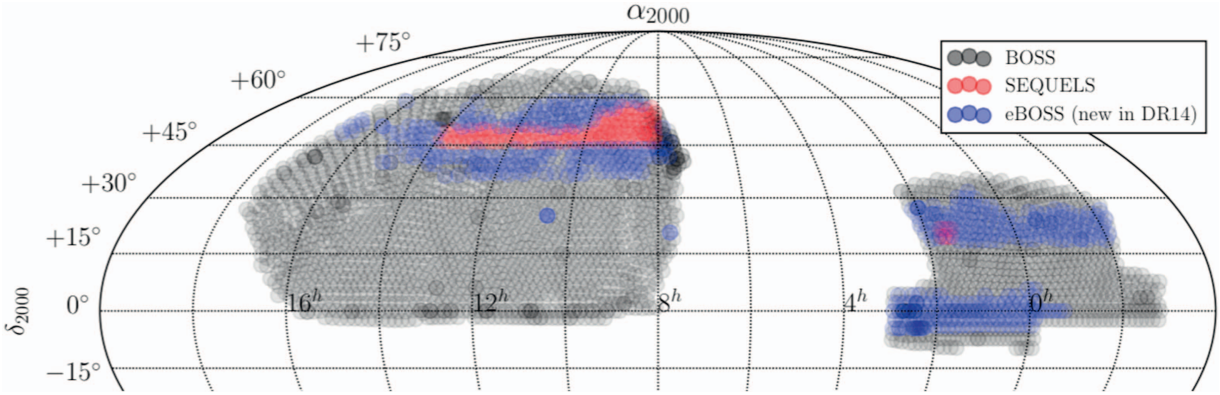

Figure 2. DR14 eBOSS spectroscopic coverage in equatorial coordinates (map centered at R.A. = 8^h.) BOSS coverage is shown in gray, SEQUELS in red, and the eBOSS data newly released for DR14 is shown in blue.

Table 3
eBOSS Spectroscopic Target Categories in DR14

Target Category	Target Flag	# DR14	Reference(s)
Main LRG sample	LRG1_WISE	105,764	Prakash et al. (2016)
Ancillary LRG sample	LRG1_IDROP	45	Prakash et al. (2016)
Main QSO selection	QSO1_EBOSS_CORE	154,349	Myers et al. (2015)
Variability-selected QSOs	QSO1_VAR_S82	10,477	Palanque-Delabrouille et al. (2016)
	QSO1_PTF	54,037	Myers et al. (2015)
Re-observed BOSS QSOs	QSO1_REOBS	16,333	Myers et al. (2015)
	QSO1_BAD_BOSS	584	
QSOs from FIRST survey	QSO1_EBOSS_FIRST	1792	Myers et al. (2015)
All eBOSS QSOs also in BOSS	QSO_BOSS_TARGET	583	Myers et al. (2015)
All eBOSS QSOs also in SDSS	QSO_SDSS_TARGET	20	Myers et al. (2015)
All "known" QSOs	QSO_KNOWN	11	Myers et al. (2015)
Time-domain spectroscopic survey (TDSS)	TDSS_TARGET	39,748	Morganson et al. (2015), MacLeod et al. (2017)
X-ray sources from RASS & *XMM-Newton*	SPIDERS_TARGET	13,261	Clerc et al. (2016), Dwelly et al. (2017)
X-ray sources in Stripe 82	S82X_TILE1	2775	LaMassa et al. (2017)
	S82X_TILE2	2621	
	S82X_TILE3	4	
ELG Pilot Survey	ELG_TEST1	15,235	Delubac et al. (2017), Raichoor et al. (2016)
	ELG1_EBOSS	4741	
	ELG1_EXTENDED	659	
Standard stars	STD_FSTAR	8420	Dawson et al. (2016)
Standard white dwarfs	STD_WD	546	Dawson et al. (2016)

spectra. We find that a S/N per pixel of around 20 (5) allows a statistical accuracy on $\log_{10}(M^*/M_\odot)$ of 0.2 (0.4) dex for the Chabrier IMF. We publish all catalogs of properties as well as model spectra of the continuum for these galaxies[141] (Comparat et al. 2017). This catalog is about twice as large as its predecessors (DR12) and will be useful for a variety of studies on galaxy evolution and cosmology.

4.4.1. The SDSS-DR14 Quasar Catalog

Following the tradition established by SDSS-I/-II/-III, the SDSS-IV/eBOSS collaboration is producing a visually inspected quasar catalog. The SDSS-DR14 quasar catalog (DR14Q; Pâris et al. 2017b) is the first to be released that contains new identifications that are mostly from eBOSS. The contents of this are similar to the DR12 version (which contained final data from BOSS as well as data from the preliminary eBOSS survey "SEQUELS") as described in Pâris et al. (2017a).

[141] https://www.sdss.org/dr14/spectro/eboss-firefly-value-added-catalog

4.4.2. Composite Spectra of BOSS Quasars Binned on Spectroscopic Parameters from DR12Q

We present high S/N composite spectra of quasars over the redshift range $2.1 \leqslant z \leqslant 3.5$. These spectra, based on the DR12 BOSS quasar catalog (Alam et al. 2015), are binned by luminosity, spectral index, and redshift. As discussed in Jensen et al. (2016), these composite spectra can be used to reveal spectral evolution while holding luminosity and spectral index constant. These composite spectra allow investigations into quasar diversity and can be used to improve the templates used in redshift classification. See Jensen et al. (2016) for more details.

4.4.3. SPIDERS X-Ray Galaxy Cluster Catalog for DR14

A substantial fraction of SPIDERS fibers target red-sequence galaxies in candidate X-ray galaxy clusters. The systems were found by filtering X-ray photon overdensities in the *ROSAT* All-Sky Survey (RASS) with an optical cluster finder (see Clerc et al. 2016 for details on the samples and targeting strategy). Adding together the DR14 eBOSS sky area with the

SEQUELS area (Figure 1), 573 of these systems showing a richness $\lambda_{OPT} > 30$ have been completely observed as part of DR14. A complete observation means that all tiled galaxies in a cluster red sequence have a spectrum in DR14; these clusters must also contain at least one redshift from SDSS-I to -IV in their red sequence. Systems located at a border of the DR14 footprint, but in the interior of the full eBOSS footprint, will be fully covered through later observations by overlapping plates.

A total of 9029 valid redshifts were associated with these candidate rich galaxy clusters, leading to a median number of 15 redshifts per red sequence. An automated algorithm performed a preliminary membership assignment and interloper removal based on standard iterative σ-clipping method. The results of the algorithm were visually inspected by eight experienced galaxy cluster observers, ensuring at least two independent evaluators per system. A Web-based interface was specifically developed for this purpose: using as a starting point the result of the automated algorithm, the tool allows each inspector to interactively assess membership based on high-level diagnostics and figures (see Figure 16 in Clerc et al. 2016). A final decision is made by each evaluator whether to validate the system as a bona fide galaxy cluster or "unvalidate" the system by lack of data or identification of a false candidate. Validation is in most cases a consequence of finding three or more red-sequence galaxies in a narrow redshift window, compatible with them all being galaxy cluster members. A robust weighted average of the cluster member redshifts provides the cluster systemic redshift. A majority vote was required for each system to be finally "validated" or "unvalidated"; in the former case, an additional condition for agreement is the overlap of the cluster redshifts' 95% confidence intervals. A second round of evaluations involving four inspectors per system was necessary to resolve cases with no clear majority.

In total, 520 of these systems are validated as true galaxy clusters based on spectroscopic data, and they form the SPIDERS X-ray galaxy cluster VAC for DR14. Among them, 478 are unique components along a line of sight. A total of 7352 spectroscopic galaxies are members of a galaxy cluster. This catalog in particular lists each galaxy cluster redshift and its uncertainty, its number of spectroscopic members, and its X-ray luminosity, assuming each component along a line of sight contributes the flux measured in RASS data.

4.4.4. The Brightest Cluster Galaxy (BCG) Properties of SPIDERS X-Ray Galaxy Clusters

We provide the BCG catalog for the SPIDERS DR14 X-ray-detected galaxy clusters VAC (see Section 4.4.3). BCGs have been identified based on the available spectroscopic data from SPIDERS and photometric data from SDSS (G. Erfanianfar et al. 2018, in preparation). Only those SPIDERS clusters that have one component in the SPIDERS X-ray galaxy clusters are considered in this analysis. Stellar masses and star formation rates (SFRs) of the BCGs are computed by combining SDSS, *WISE* (Lang 2014; Lang et al. 2014; Meisner et al. 2017), and *GALEX* (Budavári et al. 2009) photometry and using state-of-the-art spectral energy distribution (SED) fitting (Arnouts et al. 1999; Ilbert et al. 2006). Where available, the SFR is taken from the MPA-JHU galaxy properties VAC (Brinchmann et al. 2004) instead of from the SED fitting. The structural properties (effective radius, Sérsic index, axis ratio, and integrated magnitude) for all BCGs are provided by Sérsic profile fitting using SIGMA (Kelvin et al. 2012) in three optical bands (g, r, and i; Furnell et al. 2018). This catalog lists the BCGs identified as part of this process, along with their stellar mass, SFRs, and structural properties.

4.4.5. Multiwavelength Properties of RASS and XMMSL AGNs

In these two VACs, we present the multiwavelength characterization over the area covered by the SEQUELS and eBOSS DR14 surveys (2500 deg^2) of two highly complete samples of X-ray sources:

1. The *ROSAT* All-Sky Survey (RASS) X-ray source catalog (2XRS; Boller et al. 2016)
2. The *XMM-Newton* Slew Survey point source catalog (XMMSL; Saxton et al. 2008; version 1.6).

We provide information about the X-ray properties of the sources as well as of their counterparts at longer wavelengths (optical, IR, radio) identified first in the All-WISE IR catalog[142] via a Bayesian cross-matching algorithm (Dwelly et al. 2017; Salvato et al. 2018). We complement this with dedicated visual inspection of the SDSS spectra, providing accurate redshift estimates (with objective confidence levels) and source classification, beyond the standard eBOSS pipeline results.

5. APOGEE-2

DR14 is the fourth release from the Apache Point Observatory Galactic Evolution Experiment (APOGEE). DR14 presents, for the first time, the first two years of SDSS-IV APOGEE-2 data (2014 July–2016 July) as well as re-processed data from SDSS-III APOGEE-1 (2011 August–2014 July). Note that the general term APOGEE data, employed throughout this paper, refers to both APOGEE-1 and APOGEE-2 data. APOGEE-2 data are substantively the same as APOGEE-1 data; however, one of the three detectors in the instrument was replaced at the end of APOGEE-1 because it exhibited a substantial amount of persistence (i.e., light from previous exposures led to excess recorded charge in subsequent exposures). The new detector is substantially better in this regard.

APOGEE data in DR14 includes visit-combined spectra as well as pipeline-derived stellar atmospheric parameters and individual elemental abundances for 263,444 stars,[143] sampling all major components of the Milky Way. The DR14 coverage of APOGEE data is shown in Galactic coordinates in Figure 3. In addition to the Milky Way bulge, disk, and halo, DR14 includes, for the first time, data from stars in satellite galaxies, which are typically fainter targets than those from the main portion of the survey. DR14 incorporates a few modifications in the DRP as well as in the APOGEE Stellar Parameter and Chemical Abundance Pipeline (ASPCAP). It also includes a separate set of stellar parameters and abundances from The Cannon (Ness et al. 2015).[144]

Two separate papers will provide more in-depth discussion and analysis of APOGEE data released in DR13/DR14: J. Holtzman et al. (2018, in preparation) describes in detail the DR13/DR14 pipeline processing as well as the associated data

[142] http://wise2.ipac.caltech.edu/docs/release/allwise/

[143] The figure of 263,444 results from the removal of duplicate observations for a single star. Note that DR14 has a total of 277,731 entries.

[144] Named in recognition of the stellar classification work of Annie-Jump Cannon (Cannon & Pickering 1918).

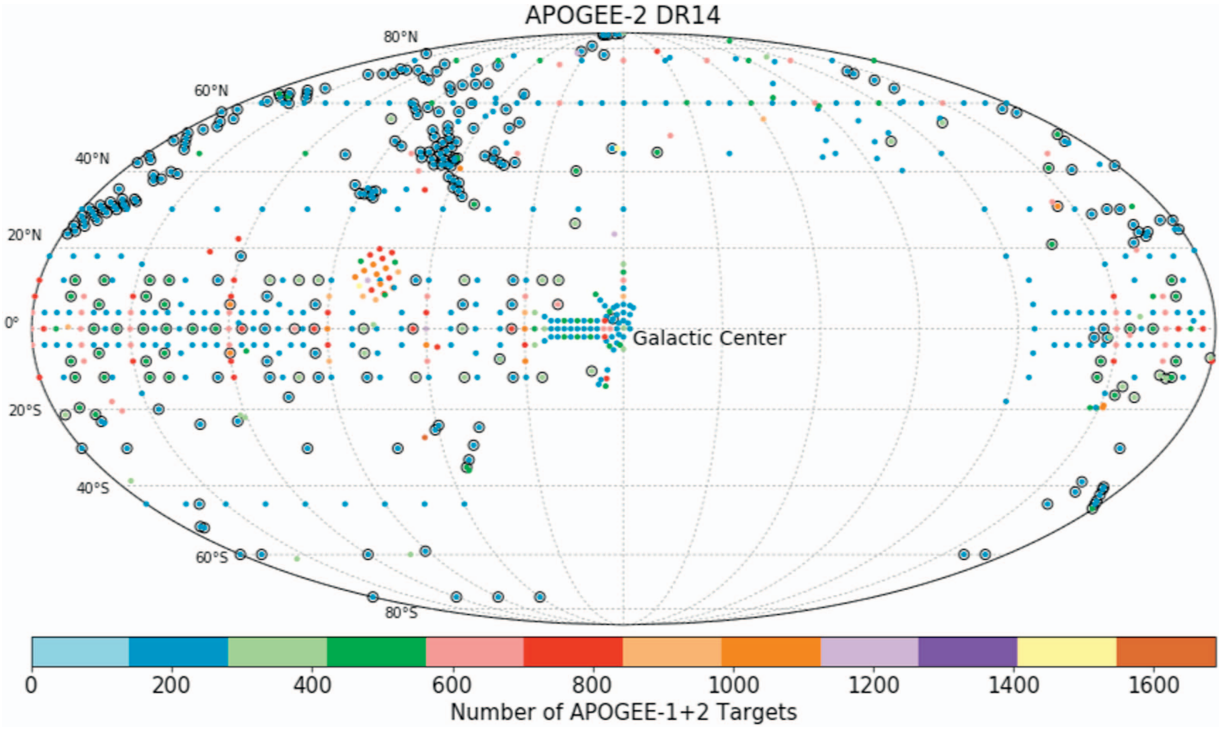

Figure 3. DR14 APOGEE spectroscopic coverage in Galactic coordinates (map centered on the Galactic center). The color coding indicates the number of APOGEE-1 +2 targets observed per field, as shown in the key. Fields new to DR14 are outlined in black.

products, and H. Jönsson et al. (2018, in preparation) compares stellar parameter and element abundances from DR13/DR14 with those from the literature.

5.1. Targeting

The targeting strategy of APOGEE-2 departs slightly from that of APOGEE-1 and is set based on a three-tier priority scheme: core, goal, and ancillary science (Zasowski et al. 2017). The core science targets, which are the highest priority, are those that directly address the primary objectives of APOGEE and include the Galactic bulge, disk, and halo; globular and open clusters; *Kepler* field spectroscopic follow-up; and satellite galaxies (unique in APOGEE-2). "Goal" science targets fall in line with APOGEE science goals with a second-tier prioritization and include M dwarfs, eclipsing binaries, substellar companions, *Kepler* Objects of Interest, young (star-forming) clusters, and Extended *Kepler* Mission (K2) spectroscopic follow-up. The third-tier priority are ancillary science targets, for which a general solicitation was issued for programs that could harness the unique capability of the APOGEE instrument.

Since the ancillary programs of APOGEE-1 were largely successful and broadened its scientific scope, APOGEE-2 continues in this vein and DR14 presents some of the first ancillary program data. As in APOGEE-1, the primary stellar targets of APOGEE-2 are red giant branch stars. APOGEE-2 extends the target stellar classes with designated observations of red-clump (RC) stars in the bulge as well as faint stars (e.g., dwarf spheroidal and halo stream members with $H \geqslant 14$). On top of the APOGEE-led programs, additional data are collected with the MaNGA co-targeting program. For the MaNGA pointings, APOGEE data are collected concurrently, with the targeted fields in the direction of the Galactic caps. To document the APOGEE-2 targeting scheme, a new set of bit flags is employed in DR14: `APOGEE2_TARGET1`, `APOGEE2_TARGET2`, and `APOGEE2_TARGET3`. Further details with regard to the APOGEE-2 targeting strategy and field design may be found in Zasowski et al. (2017), including information on APOGEE-2S targets, which are planned to be part of the next data release.

5.2. Reduction and Analysis Pipeline. Data Products

As with the previous data releases, all spectra are processed through the DRP, which includes dark current subtraction, cosmic-ray removal, flat-fielding, spectral extraction, telluric correction, wavelength calibration, and dither combination. Radial velocities (RVs) are determined for each individual visit and the individual visit spectra are resampled to rest wavelength and combined to generate a single spectrum for each object. Associated DRP data products are the visit-combined spectra and RV values. For DR14, modifications to the RV determination and associated star combination have occurred. The RV values are now determined both relative to the combined spectrum (in an iterative fashion) as well as to the best-matching model. The RVs from the method that yields the lower scatter are adopted (`VHELIO_AVG`), and estimates of the associated error and scatter are generated. Note that the new methodology has resulted in improved RV determinations for low S/N observations (and consequently, faint stars), but there can still be potentially significant issues with some of the faintest targets. The distribution of S/N values for spectra released in DR14 (compared to those released in DR13; Albareti & Allende Prieto et al. 2017) are shown in Figure 4.

5.2.1. Persistence

As discussed in Nidever et al. (2015) and Holtzman et al. (2015), one of the three APOGEE-1 detectors (the "blue"

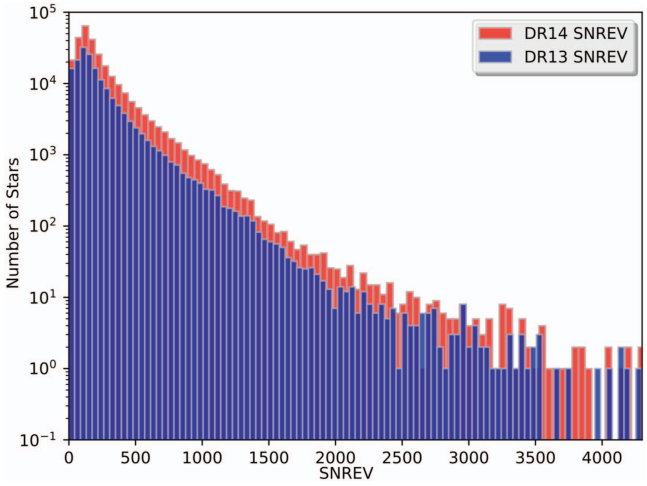

Figure 4. Comparison of the S/N distribution of APOGEE spectra released in DR14 (red) with those released in DR13 (blue). The S/N quantity displayed in the figure is SNREV, a revised S/N estimate that considers persistence issues.

detector) exhibited significant levels of persistence (i.e., charge that is held between exposures) over one-third of the detector area, and another (the "green" detector) exhibited persistence at a somewhat lower level over a smaller area. This persistence affected the derived stellar abundances (Holtzman et al. 2015). As mentioned above, the "blue" detector was replaced for APOGEE-2 in part to solve this problem. For the APOGEE-1 data, we attempt to subtract out persistence based on a model and also de-weight pixels affected by persistence during visit combination in such a way that for stars with a mix of persistence-affected and non-persistence-affected visits, the combined spectra are dominated by the non-affected visits. This results in a reduction of the systematic errors, but a slight increase of the random errors. This process significantly reduces the impact of persistence (J. Holtzman et al. 2018, in preparation); however, it can still have an effect, especially for fainter targets. Users of the APOGEE spectra should pay careful attention to the pixel-level data flags and the pixel uncertainties.

5.2.2. ASPCAP

After the DRP stage, the visit-combined stellar spectra are processed by ASPCAP, which derives the stellar atmospheric parameters (e.g., effective temperature $T\mathrm{eff}$, surface gravity $\log g$, metallicity $[M/H]$) as well as abundances for more than 20 species. The ASPCAP determination proceeds in three stages: an initial pass through ASPCAP gives coarse values for a few key atmospheric parameters to identify which spectral grids should be used on each object, a second pass yields the full set of parameters, and a final pass determines the abundances for each element with the stellar parameters fixed.

For DR14, ASPCAP modifications include a new normalization scheme for both observed and synthetic spectra. Rather than using an iteratively asymmetrically clipped fit, the continuum is determined by a polynomial fit to the spectra after masking of sky lines. This new scheme avoids clipping, since it leads to systematic differences in continuum normalization as a function of S/N. Another change is that the ASPCAP parameter determination was done by χ^2 minimization over a seven-dimensional grid for giants which included a microturbulence dimension. This leads to a slightly lower abundance scatter in clusters as well as smaller trends of $[M/H]$ with temperature.

One caveat of the DR14 ASPCAP analysis is that new grids were not constructed for APOGEE-2 line spread functions (LSFs): grids made with the APOGEE-1 LSFs were used. Since the only change was the detector replacement, large LSF changes were neither expected nor noticed, but subtle differences may be present.

5.2.3. Calibration and Data Product Usage

As with previous DRs, DR14 includes a post-ASPCAP calibration of the final stellar atmospheric parameter and element abundances. A variety of different stellar clusters and standards are employed in the calibration of the results. These calibrations include a metallicity-dependent temperature correction, a surface gravity calibration based on asteroseismic gravities, an internal and external calibration of metallicity ($[M/H]$), and a temperature-dependent and zero-point calibration for elemental abundances. Note that surface gravity calibration is not done for dwarfs because we do not have independent estimates of surface gravities from which to derive such calibrations. Calibrations are applied to abundances over temperature ranges that are determined by looking at the ranges over which data in star clusters produce the same abundance. Based on cluster results and inspection of the spectra, we do not provide calibrated abundances for Cu, Ge, Y, Rb, and Nd since these do not appear to be reliable.

Several different bitmasks (`STARFLAG`, `PARAMFLAG`, `ASPCAPFLAG`) that provide information on factors that affect data quality are included, and users are strongly encouraged to pay attention to these.

5.3. New DR14 Data Product: Results from The Cannon

New in DR14 is the inclusion of parameters and abundances derived from The Cannon (Ness et al. 2015). The Cannon is a data-driven model that provides parameters and abundances (collectively called labels) from the spectra, after training the sensitivity of each pixel to parameters and abundances based on a training set with independently derived labels.

For DR14, we train The Cannon on ASPCAP results for a subset of high S/N giant stars, and apply the model to all objects within the range of parameters covered by the training set. DR14 Cannon results have been derived using the Cannon-2 code (Casey et al. 2016), but with a few modifications. First, we adopted uncertainties from the ASPCAP pipeline, which do a better job de-weighting areas around imperfectly subtracted sky lines.

Second, and more importantly, we use "censoring" in the derivation of individual elemental abundances, which forces the model to only use pixels where there are known lines of a given element (rather than the full spectrum) to derive the abundance of that element. This was done because it was discovered that, when using the full spectrum, pixels without known lines of an element (and sometimes, with known lines of another element) contributed to the model sensitivity for that element. This suggests that the model may be affected by correlations of abundances within the training set stars. Without censoring, such correlations can lead to abundances that appear to be of higher precision, but this precision may not reflect higher accuracy, if the correlations are not present over the entire data set. While results for some elements with censoring

show less scatter than ASPCAP results, results for other elements can look significantly worse. The implementation of censoring was done by using the elemental windows used by the ASPCAP analysis; it is possible that this is overly conservative because the ASPCAP windows reject regions in the spectrum that have abundance sensitivity if they are also sensitive to other abundances in the same elemental abundance group.

5.4. APOGEE VACs

Three APOGEE-related VACs are included in DR14. They are briefly summarized below. For more details, we refer the reader to the relevant paper in Table 2.

5.4.1. DR14 APOGEE Red-clump Catalog

DR14 contains an updated version of the APOGEE red-clump (APOGEE-RC) catalog. This catalog is created using the same procedure as the original APOGEE-RC catalog (Bovy et al. 2014) now applied to the ASPCAP parameters derived in this data release. To account for changes in how the ASPCAP-derived $\log g$ is calibrated in DR14, we have made the upper $\log g$ cut more stringent by 0.1 dex (the upper $\log g$ limit in Equation (2) in Bovy et al. 2014 now has 2.4 instead of 2.5). Like in the original release, we also apply an additional $\log g$ cut to remove further contaminants (Equation (9) in Bovy et al. 2014). Otherwise, the catalog is created in the same manner as the original catalog.

The DR14 APOGEE-RC catalog contains 29,502 unique stars, about 50% more than in DR13. Note that because of changes in the target selection in APOGEE-2, the relative number of RC stars in APOGEE-2 is smaller than in APOGEE-1. We provide proper motions by matching to the UCAC-4 (Zacharias et al. 2013) and HSOY (Altmann et al. 2017) catalogs. Contamination by non-RC stars in the DR14 RC catalog is estimated to be less than 5% by comparing against true RC stars in the APOKASC catalog Pinsonneault et al. (2018).

5.4.2. DR14 APOGEE-TGAS Catalog

The first data release of the *Gaia* mission contains improved parallaxes and proper motions for more than 2 million stars contained in the Tycho-2 catalog, among them 46,033 objects (10,250 of them unique stars) contained in APOGEE DR14. This is known as the Tycho-*Gaia* Astrometric Solution (TGAS). We provide the cross-matched catalog, together with precise combined astrometric/spectrophotometric distances and extinctions determined with `StarHorse` (Queiroz et al. 2018), for 29,661 stars. We also include orbital parameters calculated using the `GravPot16` code[145] (J. Fernandez-Trincado et al. 2018, in preparation). For more details, see F. Anders et al. (2018, in preparation); a summary is also provided in Anders et al. (2017).

5.4.3. APOGEE DR14 Distance Estimations from Four Groups

This VAC provides spectrophotometric distance estimates for APOGEE stars that have been calculated by four groups, using slightly different isochrone techniques. All groups used the DR14-calibrated ASPCAP stellar parameters, if they fall inside the calibration ranges (see J. Holtzman et al. 2018, in preparation). The distances come from (1) the `StarHorse` code (Santiago et al. 2016; Queiroz et al. 2018), (2) the code described in Wang et al. (2016), (3) the isochrone-matching technique described in Schultheis et al. (2014), and (4) the distance code described in J. Holtzman et al. (2018, in preparation).

6. MaNGA

In the context of the MaNGA Survey, DR14 roughly doubles the sample size of the associated data products that were first made public in DR13. Spanning observations from the first two years of operations, the DR14 products include raw observations, intermediate reduction output, such as reduced fiber spectra, and final data cubes as constructed by the DRP (Law et al. 2016, hereafter L16). A summary `drpall` catalog provides target identification information, sky positions, and object properties like photometry and redshifts. The MaNGA observing strategy is described in Law et al. (2015), and the flux calibration scheme is presented in Yan et al. (2016b). An overview of the survey execution strategy and data quality is provided in Yan et al. (2016a). Weijmans & MaNGA Team (2016) provide a short summary to the entire survey, which is comprehensively described in Bundy et al. (2015).

DR14 includes observations from 166 MaNGA plates resulting in 2812 data cubes comprising targets in the main samples as well as ancillary programs, and around 50 repeat observations. The sky layout of the DR14-released MaNGA data is shown in Figure 5.

6.1. MaNGA Target Classes

The target selection for the MaNGA Survey is described in detail by Wake et al. (2017). MaNGA's main galaxy sample contains galaxies with stellar masses $M_* > 10^9\,M_\odot$ and is comprised of three main subsamples that are defined on the basis of SDSS-I/-II photometry and spectroscopic redshifts to deliver a final distribution that is roughly flat in $\log M_*$. The Primary sample achieves radial coverage out to 1.5 times the effective radii (1.5 R_e) for target galaxies, while the Secondary sample reaches 2.5 R_e. The Color-enhanced supplement expands the selection of the Primary sample to include underrepresented regions of M_*–color space. We refer to the combination of the Primary and Color-enhanced supplements as "Primary+," which balances the rest-frame color distribution at fixed M_*. The MaNGA samples can be weighted so that they are equivalent to a volume-limited sample. The required volume weights are described in Wake et al. (2017) and are provided in the DR14 version of the targeting file.

DR14 includes 1278 Primary galaxies, 947 Secondary galaxies, and 447 Color-enhanced supplement galaxies. Which sample a given target galaxy belongs to is given by the MANGA_TARGET1 bitmask (or mngtarg1 in the "drpall" file). Bits 10, 11, and 12 signal that galaxies were selected as Primary, Secondary, or Color-Enhanced targets, respectively. In addition to ∼121 ancillary program targets, ∼50 galaxies were observed as fillers and do not fall into these target categories. They should be ignored in statistical studies of the MaNGA data.

MaNGA has also begun observing Milky Way stars in a bright-time survey program called the MaNGA Stellar Library (MaStar) that makes use of MaNGA IFUs during APOGEE-2

[145] https://fernandez-trincado.github.io/GravPot16/

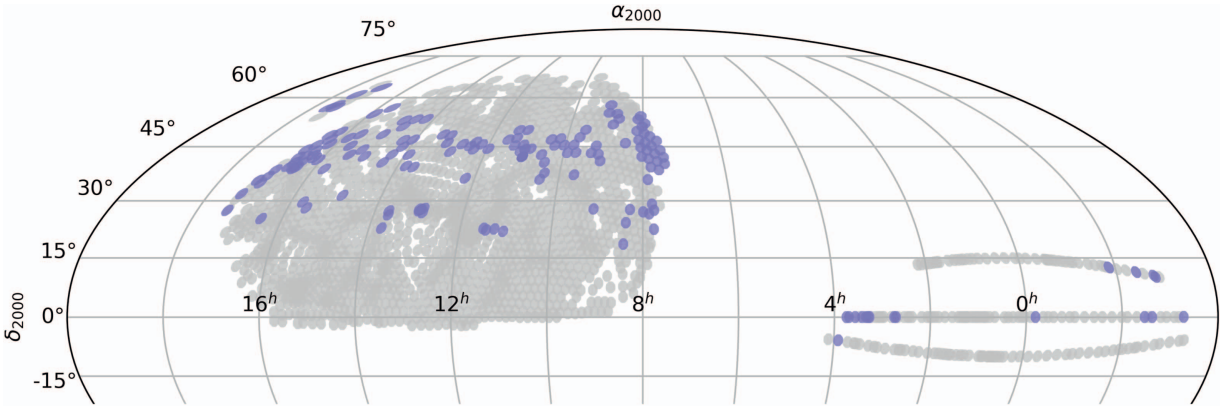

Figure 5. Sky distribution (Molleweide equatorial projection for decl. $>-20°$) of possible MaNGA plates (in light gray). Because MaNGA targets are selected from a sample with SDSS-I photometry and redshifts, this footprint corresponds to the Data Release 7 imaging data (Abazajian et al. 2009). Each plate contains 17 MaNGA targets, and around 30% of all possible plates will be observed in the full six-year survey. The dark purple indicates plates with data released as part of DR14.

observations. The goal of MaStar is to build a new stellar library comprising >8000 stars that span the widest accessible ranges in effective temperature, surface gravity, metallicity, and element abundance ratios (Yan et al. 2017; Pinsonneault et al. 2018). Reduced stellar spectra will be included in DR15.

As described in the DR13 paper, roughly 5% of MaNGA IFUs are allocated to targets defined by approved ancillary programs. These sources can be identified using the MANGA_TARGET3 bitmask (or mngtarg3 in the drpall file). Most of the programs represented in DR14 are described in DR13.[146] They include targeted follow-up of AGN hosts, starburst galaxies, merging systems, dwarf galaxies, Milky Way analogs, and BCGs. New in DR14, we include deep observations reaching ~20 hr in the center of the Coma cluster (Gu et al. 2017) and IFU observations allocated as part of an ancillary program to a nearby dwarf galaxy that is part of the ACS Nearby Galaxy Survey (Dalcanton et al. 2009).

6.2. Working with MaNGA Data

All MaNGA data products take the form of multi-extension FITS files. As we describe in DR13, the DRP data products consist of intermediate reduced data (sky-subtracted, flux-calibrated fiber spectra with red and blue data combined for individual exposures of a plate) and final-stage data products (summary row-stacked spectra and data cubes) for each target galaxy. The summary row-stacked spectra (RSS files) are two-dimensional arrays provided for each galaxy in which each row corresponds to a single fiber spectrum.

The three-dimensional data cubes are created by combining the individual spectra for a given galaxy together onto a regularized 0.″5 grid (see L16 for more details). The associated wavelength arrays for both the data cubes and RSS files can be accessed in logarithmic and linear scales. Each data cube contains additional extensions with information that includes the inverse variance, a bad-pixel mask, instrumental resolution, reconstructed broadband images, and the effective spatial point-spread function. The full data model for all MaNGA DRP data products can be found online at http://www.sdss.org/dr14/manga/manga-data/data-model and in Appendix B of L16.

[146] Also see http://www.sdss.org/dr14/manga/manga-target-selection/ancillary-targets.

The DR14 pipeline for MaNGA is nearly identical to that in DR13 with a few small exceptions listed below:

1. The spectral resolution reported is worse by about 10%. This change reflects the growing understanding of the data quality to account for the effects of both pre- versus post-pixelization Gaussian profile fitting and changes in the LSF introduced by the wavelength rectification. There are likely to be further small changes in future data releases.
2. Local reddening maps (rather than plate averages) have been used in calculations of S/N of the spectra.
3. Spaxels flagged as containing foreground stars are now ignored by the astrometric routines. This may result in some small changes in astrometry for some objects.
4. The bias calculation in the blue camera has been improved. The impact of this will be negligible, except to improve the quality of some extremely bright emission lines.
5. Adjustments were made to the sky subtraction algorithms to optimize performance for the Coma cluster ancillary program.
6. There have been improvements in the data quality flagging for cubes with dead fibers.

Instructions for accessing the MaNGA data products are given on the SDSS Web site.[147] We summarize available options here and refer the reader to the DR13 paper for additional details. All data products are stored on the SAS at http://data.sdss.org/sas/dr14/manga/spectro/redux/. Here you will find the `drpall` summary table as well as the subdirectories that store the reduction output for each plate, both for observations obtained on a specific night and for the results of combining all observations of a given plate into a "stack." The drpall table may be queried either after downloading this file to disk or through the SDSS CASJobs system. Such queries define selections of galaxies of interest and can return the plate–IFU combination for those galaxies that identifies how they were observed. These in turn can be used to find the SAS directory locations of the corresponding data products. Large downloads can be accomplished via rsync calls as described on the SDSS Web site. Finally, the SDSS SkyServer Explore tool provides basic information about the MaNGA targets.

[147] http://www.sdss.org/dr14/manga/manga-data/data-access/

Several features of the MaNGA data should be kept in mind while using the data. Most important, each MaNGA data cube has a FITS header keyword DRP3QUAL indicating the quality of the reduction. One to two percent of the data cubes are flagged as significantly problematic—galaxies with CRITICAL quality bit (=30) set should be treated with extreme caution (see L16). Please also use the MASK extension of each data cube to identify problematic spaxels. A simple summary DONOTUSE bit is of particular importance, indicating elements that should be masked out for scientific analyses.

There is significant covariance between adjacent spaxels in data cubes, given that the spaxel size (0.″5) is much smaller than the fiber size (2″ diameter). A simple method that accounts for covariance when one desires to spatially bin spaxels together is discussed in Section 9.3 of L16. The typical reconstructed point-spread function of the MaNGA data cubes has an FWHM of 2.″5. Sparse correlation matrices in the *ugriz* central wavelengths are also now provided in the data cubes.

As discussed by L16, the instrumental LSF in the DR13 data was underestimated by about 10% ± 2%. This has been corrected in DR14, and the reported LSF is described by a post-pixelized Gaussian.

Additional issues and caveats are discussed in http://www.sdss.org/dr14/manga/manga-caveats/.

6.3. Highlights of MaNGA Science with DR14 Data

The MaNGA survey has produced a number of scientific results based on data acquired so far, indicating the breadth of research possible with the MaNGA data. In the DR13 paper, we provided a summary of science highlights with early data. Here, we briefly summarize the results of papers that have been completed within the SDSS-IV collaboration using the MaNGA sample released as part of DR14.

For example, published results based on the MaNGA DR14 data include Barrera-Ballesteros et al. (2017), who discuss the integrated stellar mass–metallicity relation for more than 1700 galaxies; Zhu et al. (2017), who revisit the relation between the stellar surface density, the gas surface density, and the gas-phase metallicity of typical disk galaxies in the local universe; Belfiore et al. (2017), who study the gas-phase metallicity and nitrogen abundance gradients traced by star-forming regions in a representative sample of 550 nearby galaxies; and Lin et al. (2017), who report the discovery of a mysterious giant Hα blob that is ∼8 kpc away from a component of a dry galaxy merger. Bizyaev et al. (2017) presented a study of the kinematics of the extraplanar ionized gas around several dozen galaxies, while Jones et al. (2017) conducted a detailed study of extraplanar diffuse ionized gas stacking spectra from 49 edge-on, late-type galaxies as a function of distance from the midplane of the galaxy. Numerous other results based on DR14 data are in preparation.

6.4. MaNGA VACs

This data release also contains two VACs based on MaNGA data. They are briefly summarized below, and for more details, we refer the reader to the papers given in Table 2.

6.4.1. MaNGA Pipe3D VAC: Spatially Resolved and Integrated Properties of Galaxies

PIPE3D is an IFU-focused analysis pipeline that calculates intermediate data products and is able to obtain both the stellar population and the ionized gas properties extracted from the data cubes in an automatic way. This pipeline is based on FIT3D, the details of which are presented in Sánchez et al. (2016a, 2016b), which show some examples based on CALIFA (Cano-Díaz et al. 2016; Sánchez-Menguiano et al. 2016; Sánchez et al. 2017b) and MaNGA/P-MaNGA (Barrera-Ballesteros et al. 2016; Ibarra-Medel et al. 2016; Barrera-Ballesteros et al. 2017; Lin et al. 2017) data sets. The MaNGA data products provided by Pipe3D are presented in Sánchez et al. (2017a).[148] The VAC consists of a single table containing integrated (cumulative), characteristic (values at the effective radius), and gradients of different quantities, including stellar mass, star formation (and their densities), oxygen and nitrogen abundances, dust attenuation, estimated gas density, and stellar and gas velocity dispersions.

For each galaxy, the data are presented as individual FITS files including four extensions, each one corresponding to a data cube that comprises (1) the spatial resolved properties required to recover the star formation histories, (2) the average properties of the stellar populations, (3) the emission-line properties for 56 strong and weak emission lines (including the former ones together with the equivalent width of the lines), and (4) the most frequently used stellar indices. The details of each individual extension were described in Sánchez et al. (2016b), and the final adopted format is given in Sánchez et al. (2017a).

6.4.2. MaNGA FIREFLY Stellar Populations

The MaNGA FIREFLY VAC (Goddard et al. 2017) provides measurements of spatially resolved stellar population properties in MaNGA galaxies. It is built on and complements the products of the MaNGA data analysis pipeline (DAP; K. Westfall et al. 2018, in preparation) by providing higher order and model-based data products. These are measurements of optical absorption line strengths as well as the physical properties age, metallicity, and dust attenuation. The latter are derived from full spectral fitting with the code FIREFLY (Wilkinson et al. 2015, 2017) using the supercomputer SCIAMA2 at Portsmouth University. The VAC is a single FITS file (4 GB) containing measurements of all DR14 MaNGA galaxies. The catalog contains basic galaxy information from the literature (i.e., galaxy identifiers, redshift, mass), global derived parameters (i.e., light-weighted and mass-weighted stellar population ages and metallicities for a central 3 arcsec aperture and for an elliptical shell at 1 effective radius), gradient parameters (i.e., gradients in age and metallicity measured within 1.5 R_e), and spatially resolved quantities (i.e., 2D maps of age, metallicity, dust attenuation, mass and surface mass density, and 28 absorption line indices).

More details on the catalog and the method for creating the two-dimensional maps are provided in Goddard et al. (2017), and the data are available from the data release Web site.[149]

7. Future Plans

SDSS-IV is planning a six-year survey, with operations at both the 2.5 m Sloan Foundation Telescope at APO, New Mexico, USA, and the du Pont Telescope at Las Campanas,

[148] http://www.sdss.org/dr14/manga/manga-data/manga-pipe3d-value-added-catalog

[149] http://www.sdss.org/dr14/manga/manga-data/manga-firefly-value-added-catalog

Chile, scheduled through 2020. Future data releases from SDSS-IV will include data observed with both telescopes; the final SDSS-IV data release is planned to be DR18, currently scheduled for 2020 December.

For APOGEE, future data releases will include, for the first time, southern hemisphere observations taken with the new APOGEE-S instrument at the Las Campanas Observatory with the du Pont 2.5 m telescope. These observations will extend APOGEE coverage to the full Galaxy, with significantly increased observations of the Galactic bulge and also include observations in the Magellanic Clouds, globular clusters, and dwarf spheroidal galaxies only accessible from the southern hemisphere. As usual, future data releases will also include re-reductions of all APOGEE-N data. Plans for improved stellar parameter/abundance analysis include using a new homogeneous grid of MARCS stellar atmospheres and the use of "minigrids" to analyze elements whose absorption features are too blended with those of other elements to be reliably extracted with the abundance techniques used to date.

For MaNGA, it is planned that the DR15 data release will include the ~4000 MaNGA galaxies that have been observed up to the summer shutdown of 2017. In addition, we anticipate a number of new data products to be released in this and future DRs. These include reduced spectra from the MaStar stellar library (Yan et al. 2017), which is making use of commensal observations during APOGEE-2 time to obtain spectroscopic observations of stars which will be used to build a new stellar library through the MaNGA instrumentation, and output from the MaNGA DAP (K. Westfall et al. 2018, in preparation). The DAP produces maps of emission-line fluxes, gas and stellar kinematics, and stellar population properties. Some similar derived data products are already available as VACs (see Table 2 and Sections 6.4.1 and 6.4.2). Finally, we intend for DR15 to mark the first release of the "Marvin" ecosystem, which includes powerful Python tools for seamlessly downloading and querying the MaNGA data as well as a Web interface that provides advanced search functionality, a user interface for the MaNGA data cubes, and the ability to quickly choose and display maps of key quantities measured by the DAP.

For eBOSS, future data releases will include the ELG survey results as well as the continuation of the LRG-QSO surveys. They will also include further VACs: in particular, the continuation of the quasar catalog, a detailed ELG catalog, as well as large-scale structure clustering catalogs required for independent clustering analysis. Further improvement on the redshift measurement and spectral classification catalog is also likely.

For TDSS, a future SDSS data release will include very recent spectra from its Repeat Quasar Spectroscopy (RQS) program, which obtains multi-epoch spectra for thousands of known quasars, all of which have least one epoch of SDSS spectroscopy available (and often already archived). Quasar spectral variability on multiyear timescales is currently poorly characterized for large samples, although there are many exciting results from smaller select subsets (see Runnoe et al. 2016 and McGraw et al. 2017 for examples of studies based on repeat spectroscopy, ranging from discoveries of new changing-look quasars to BAL emergence and disappearance). The RQS program in TDSS will ultimately observe $\sim 10^4$ known (SDSS) quasars in the ELG survey region (Raichoor et al. 2017), adding at least one additional spectral epoch. This will allow for an extension of earlier work to a systematic investigation of quasar spectroscopic variability, both by making a larger sample and also by including large numbers of quasars as targets for repeat spectra that were selected without a priori knowledge of their specific quasar spectroscopic subclass or variability properties. A recent detailed technical description of target selection for all of the TDSS repeat spectroscopy programs (including RQS) may be found in MacLeod et al. (2017).

For SPIDERS, future data releases will focus on higher level data products, such as black hole masses and host galaxy properties of the X-ray AGN, as well as rich characterization of the X-ray-selected clusters (in particular, dynamical properties and calibrated cluster masses). The first spectra of counterparts of eROSITA sources, however, will only be obtained beginning in spring 2019, so they will be part of DR18 and subsequent releases only.

Planning has begun for the next generation of SDSS, to begin in 2020 (Kollmeier et al. 2017). SDSS-V will build on the SDSS infrastructure and expand the instrumentation (especially for optical IFU spectroscopy) in both hemispheres. This expansion of SDSS's legacy will enable an enormous sample comprising millions of spectra of quasars, galaxies, and stars, with scientific goals ranging from the growth of supermassive black holes to the chemical and dynamical structure of the Milky Way, the detailed architecture of planetary systems, and the astrophysics of star formation.

We would like to thank the University of St Andrews, Scotland, for their hospitality during DocuCeilidh 2017.

Funding for the Sloan Digital Sky Survey IV has been provided by the Alfred P. Sloan Foundation, the U.S. Department of Energy Office of Science, and the Participating Institutions. SDSS-IV acknowledges support and resources from the Center for High-Performance Computing at the University of Utah. The SDSS web site is www.sdss.org.

SDSS-IV is managed by the Astrophysical Research Consortium for the Participating Institutions of the SDSS Collaboration, including the Brazilian Participation Group, the Carnegie Institution for Science, Carnegie Mellon University, the Chilean Participation Group, the French Participation Group, Harvard-Smithsonian Center for Astrophysics, Instituto de Astrofísica de Canarias, The Johns Hopkins University, Kavli Institute for the Physics and Mathematics of the Universe (IPMU)/University of Tokyo, Lawrence Berkeley National Laboratory, Leibniz Institut für Astrophysik Potsdam (AIP), Max-Planck-Institut für Astronomie (MPIA Heidelberg), Max-Planck-Institut für Astrophysik (MPA Garching), Max-Planck-Institut für Extraterrestrische Physik (MPE), National Astronomical Observatories of China, New Mexico State University, New York University, University of Notre Dame, Observatário Nacional/MCTI, The Ohio State University, Pennsylvania State University, Shanghai Astronomical Observatory, United Kingdom Participation Group, Universidad Nacional Autónoma de México, University of Arizona, University of Colorado Boulder, University of Oxford, University of Portsmouth, University of Utah, University of Virginia, University of Washington, University of Wisconsin, Vanderbilt University, and Yale University.

ORCID iDs

Carlos Allende Prieto https://orcid.org/0000-0002-0084-572X
Brett H. Andrews https://orcid.org/0000-0001-8085-5890

Borja Anguiano https://orcid.org/0000-0001-5261-4336
Alfonso Aragón-Salamanca https://orcid.org/0000-0001-8215-1256
Vladimir Avila-Reese https://orcid.org/0000-0002-3461-2342
Carles Badenes https://orcid.org/0000-0003-3494-343X
Kathleen A. Barger https://orcid.org/0000-0001-5817-0932
Jorge Barrera-Ballesteros https://orcid.org/0000-0003-2405-7258
Rachael Beaton https://orcid.org/0000-0002-1691-8217
Timothy C. Beers https://orcid.org/0000-0003-4573-6233
Francesco Belfiore https://orcid.org/0000-0002-2545-5752
Chad F. Bender https://orcid.org/0000-0003-4384-7220
Matthew A. Bershady https://orcid.org/0000-0002-3131-4374
Guillermo A. Blanc https://orcid.org/0000-0003-4218-3944
Michael R. Blanton https://orcid.org/0000-0003-1641-6222
Jura Borissova https://orcid.org/0000-0002-5936-7718
Jo Bovy https://orcid.org/0000-0001-6855-442X
William Nielsen Brandt https://orcid.org/0000-0002-0167-2453
Joel R. Brownstein https://orcid.org/0000-0002-8725-1069
Kevin Bundy https://orcid.org/0000-0001-9742-3138
Adam J. Burgasser https://orcid.org/0000-0002-6523-9536
Mariana Cano-Díaz https://orcid.org/0000-0001-9553-8230
Michele Cappellari https://orcid.org/0000-0002-1283-8420
Ricardo Carrera https://orcid.org/0000-0001-6143-8151
Andrew R. Casey https://orcid.org/0000-0003-0174-0564
Yanping Chen https://orcid.org/0000-0001-8821-0309
Drew Chojnowski https://orcid.org/0000-0001-9984-0891
Haeun Chung https://orcid.org/0000-0002-3043-2555
Kevin Covey https://orcid.org/0000-0001-6914-7797
Jeffrey D. Crane https://orcid.org/0000-0002-5226-787X
Jeremy Darling https://orcid.org/0000-0003-2511-2060
Kyle Dawson https://orcid.org/0000-0002-0553-3805
Nathan De Lee https://orcid.org/0000-0002-3657-0705
Flavia Dell'Agli https://orcid.org/0000-0003-2442-6981
Niv Drory https://orcid.org/0000-0002-7339-3170
Eric Emsellem https://orcid.org/0000-0002-6155-7166
Michael Eracleous https://orcid.org/0000-0002-3719-940X
Xiaohui Fan https://orcid.org/0000-0003-3310-0131
Diane Feuillet https://orcid.org/0000-0002-3101-5921
Scott W. Fleming https://orcid.org/0000-0003-0556-027X
Peter Frinchaboy https://orcid.org/0000-0002-0740-8346
Lluís Galbany https://orcid.org/0000-0002-1296-6887
Ana E. García Pérez https://orcid.org/0000-0003-2184-6198
Patrick Gaulme https://orcid.org/0000-0001-8330-5464
Joseph Gelfand https://orcid.org/0000-0003-4679-1058
Violeta Gonzalez-Perez https://orcid.org/0000-0001-9938-2755
Paul J. Green https://orcid.org/0000-0002-8179-9445
Catherine J. Grier https://orcid.org/0000-0001-9920-6057
Hong Guo https://orcid.org/0000-0003-4936-8247
Alex Hagen https://orcid.org/0000-0003-2031-7737
Paul Harding https://orcid.org/0000-0003-3442-6248
Suzanne Hawley https://orcid.org/0000-0002-6629-4182
Fred Hearty https://orcid.org/0000-0002-1664-3102
Saskia Hekker https://orcid.org/0000-0002-1463-726X
Jesus Hernandez https://orcid.org/0000-0001-9797-5661
David W. Hogg https://orcid.org/0000-0003-2866-9403
Kelly Holley-Bockelmann https://orcid.org/0000-0003-2227-1322
Jon A. Holtzman https://orcid.org/0000-0002-9771-9622
Bau-Ching Hsieh https://orcid.org/0000-0001-5615-4904
Jason A. S. Hunt https://orcid.org/0000-0001-8917-1532
Jennifer A. Johnson https://orcid.org/0000-0001-7258-1834
Henrik Jönsson https://orcid.org/0000-0002-4912-8609
Eric Jullo https://orcid.org/0000-0002-9253-053X
Karen Kinemuchi https://orcid.org/0000-0001-7908-7724
Gillian R. Knapp https://orcid.org/0000-0002-9259-1164
Jean-Paul Kneib https://orcid.org/0000-0002-4616-4989
Juna A. Kollmeier https://orcid.org/0000-0001-9852-1610
Ivan Lacerna https://orcid.org/0000-0002-7802-7356
Dustin Lang https://orcid.org/0000-0002-1172-0754
David R. Law https://orcid.org/0000-0002-9402-186X
Hongyu Li https://orcid.org/0000-0002-6518-9866
Jianhui Lian https://orcid.org/0000-0001-5258-1466
Lihwai Lin (林俐暉) https://orcid.org/0000-0001-7218-7407
Sara Lucatello https://orcid.org/0000-0001-8808-0073
Britt Lundgren https://orcid.org/0000-0002-6463-2483
Suvrath Mahadevan https://orcid.org/0000-0001-9596-7983
Steven Majewski https://orcid.org/0000-0003-2025-3147
Arturo Manchado https://orcid.org/0000-0002-3011-686X
Karen L. Masters (何凱論) https://orcid.org/0000-0003-0846-9578
Ian D. McGreer https://orcid.org/0000-0002-3461-5228
Michael R. Merrifield https://orcid.org/0000-0002-4202-4727
Andres Meza https://orcid.org/0000-0002-9460-7828
Ivan Minchev https://orcid.org/0000-0002-5627-0355
Dante Minniti https://orcid.org/0000-0002-7064-099X
Kirpal Nandra https://orcid.org/0000-0002-7150-9192
Jeffrey A. Newman https://orcid.org/0000-0001-8684-2222
David L. Nidever https://orcid.org/0000-0002-1793-3689
Julia O'Connell https://orcid.org/0000-0003-2321-950X
Zach Pace https://orcid.org/0000-0003-4843-4185
Nelson Padilla https://orcid.org/0000-0001-9850-9419
Hsi-An Pan https://orcid.org/0000-0002-1370-6964
Kaike Pan https://orcid.org/0000-0002-2835-2556
Changbom Park https://orcid.org/0000-0001-9521-6397
Samantha Penny https://orcid.org/0000-0001-5703-7531
Ismael Perez-Fournon https://orcid.org/0000-0002-2807-6459
Marc Pinsonneault https://orcid.org/0000-0002-7549-7766
Abhishek Prakash https://orcid.org/0000-0003-4451-4444
M. Jordan Raddick https://orcid.org/0000-0003-0801-7360
Hans-Walter Rix https://orcid.org/0000-0003-4996-9069
Carlos Román-Zúñiga https://orcid.org/0000-0001-8600-4798
John Ruan https://orcid.org/0000-0001-8665-5523
Mara Salvato https://orcid.org/0000-0001-7116-9303
Sebastián F. Sánchez https://orcid.org/0000-0001-6444-9307
Jaderson S. Schimoia https://orcid.org/0000-0002-5640-6697
Edward Schlafly https://orcid.org/0000-0002-3569-7421
David Schlegel https://orcid.org/0000-0002-5042-5088
William J. Schuster https://orcid.org/0000-0002-0988-7491
Aldo Serenelli https://orcid.org/0000-0001-6359-2769
Shiyin Shen https://orcid.org/0000-0002-3073-5871
Yue Shen https://orcid.org/0000-0003-1659-7035

Matthew Shetrone https://orcid.org/0000-0003-0509-2656
Michael Shull https://orcid.org/0000-0002-4594-9936
Víctor Silva Aguirre https://orcid.org/0000-0002-6137-903X
Garrett Somers https://orcid.org/0000-0002-9322-0314
David V. Stark https://orcid.org/0000-0002-3746-2853
Keivan Stassun https://orcid.org/0000-0002-3481-9052
Matthias Steinmetz https://orcid.org/0000-0001-6516-7459
Dennis Stello https://orcid.org/0000-0002-4879-3519
Thaisa Storchi-Bergmann https://orcid.org/0000-0003-1772-0023
Guy S. Stringfellow https://orcid.org/0000-0003-1479-3059
Genaro Suárez https://orcid.org/0000-0002-2011-4924
Baitian Tang https://orcid.org/0000-0002-0066-0346
Jamie Tayar https://orcid.org/0000-0002-4818-7885
Daniel Thomas https://orcid.org/0000-0002-6325-5671
Patricia Tissera https://orcid.org/0000-0001-5242-2844
Nicholas W. Troup https://orcid.org/0000-0003-3248-3097
Remco van den Bosch https://orcid.org/0000-0002-0420-6159
David Wake https://orcid.org/0000-0002-6047-1010
Kyle B. Westfall https://orcid.org/0000-0003-1809-6920
W. M. Wood-Vasey https://orcid.org/0000-0001-7113-1233
Dominika Wylezalek https://orcid.org/0000-0003-2212-6045
Renbin Yan https://orcid.org/0000-0003-1025-1711
Jason E. Ybarra https://orcid.org/0000-0002-3576-4508
Nadia Zakamska https://orcid.org/0000-0001-6100-6869
Kai Zhang https://orcid.org/0000-0002-9808-3646
Zhi-Min Zhou https://orcid.org/0000-0002-4135-0977
Joel C. Zinn https://orcid.org/0000-0002-7550-7151
Hu Zou https://orcid.org/0000-0002-6684-3997

References

Abazajian, K. N., Adelman-McCarthy, J. K., Agüeros, M. A., et al. 2009, ApJS, 182, 543
Aghamousa, A., Aguilar, J., DESI Collaboration, et al. 2016a, arXiv:1611.00036
Aghamousa, A., Aguilar, J., DESI Collaboration, et al. 2016b, arXiv:1611.00037
Ahn, C. P., Alexandroff, R., Allende Prieto, C., et al. 2012, ApJS, 203, 21
Aihara, H., Allende Prieto, C., An, D., et al. 2011, ApJS, 193, 29
Alam, S., Albareti, F. D., Allende Prieto, C., et al. 2015, ApJS, 219, 12
Albareti, F. D., Allende Prieto, C., Almeida, A., et al. 2017, ApJS, 233, 25 (DR13)
Albrecht, A., Bernstein, G., Cahn, R., et al. 2006, arXiv:astro-ph/0609591
Altmann, M., Roeser, S., Demleitner, M., Bastian, U., & Schilbach, E. 2017, A&A, 600, L4
Anders, F., Queiroz, A. B., Chiappini, C., et al. 2017, in Proc. IAU Symp. 334, Rediscovering our Galaxy, ed. C. Chiappini et al. arXiv:1708.09319
Arnouts, S., Cristiani, S., Moscardini, L., et al. 1999, MNRAS, 310, 540
Ata, M., Baumgarten, F., Bautista, J., et al. 2017, arXiv:1705.06373
Barrera-Ballesteros, J. K., Heckman, T. M., Zhu, G. B., et al. 2016, MNRAS, 463, 2513
Barrera-Ballesteros, J. K., Sánchez, S. F., Heckman, T., Blanc, G. A., & The MaNGA Team 2017, ApJ, 844, 80
Bautista, J. E., Busca, N. G., Guy, J., et al. 2017, arXiv:1702.00176
Belfiore, F., Maiolino, R., Tremonti, C., et al. 2017, MNRAS, 469, 151
Bershady, M. A., Verheijen, M. A. W., Swaters, R. A., et al. 2010, ApJ, 716, 198
Bizyaev, D., Walterbos, R. A. M., Yoachim, P., et al. 2017, ApJ, 839, 87
Blake, C., Davis, T., Poole, G. B., et al. 2011, MNRAS, 415, 2892
Blanton, M. R., Bershady, M. A., Abolfathi, B., et al. 2017, AJ, 154, 28
Boller, T., Freyberg, M. J., Trümper, J., et al. 2016, A&A, 588, A103
Bovy, J., Nidever, D. L., Rix, H.-W., et al. 2014, ApJ, 790, 127
Brinchmann, J., Charlot, S., White, S. D. M., et al. 2004, MNRAS, 351, 1151
Bryant, J. J., Owers, M. S., Robotham, A. S. G., et al. 2015, MNRAS, 447, 2857
Budavári, T., Heinis, S., Szalay, A. S., et al. 2009, ApJ, 694, 1281
Bundy, K., Bershady, M. A., Law, D. R., et al. 2015, ApJ, 798, 7
Cannon, A. J., & Pickering, E. C. 1918, AnHar, 91, 1
Cano-Díaz, M., Sánchez, S. F., Zibetti, S., et al. 2016, ApJL, 821, L26
Cappellari, M., Emsellem, E., Krajnović, D., et al. 2011, MNRAS, 413, 813
Casey, A. R., Hogg, D. W., Ness, M., et al. 2016, arXiv:1603.03040
Cirasuolo, M., Afonso, J., Carollo, M., et al. 2014, Proc. SPIE, 9147, 91470N
Clerc, N., Merloni, A., Zhang, Y.-Y., et al. 2016, MNRAS, 463, 4490
Colless, M., Peterson, B. A., Jackson, C., et al. 2003, arXiv:astro-ph/0306581
Comparat, J., Maraston, C., Goddard, D., et al. 2017, A&A, submitted (arXiv:1711.06575)
Cui, X.-Q., Zhao, Y.-H., Chu, Y.-Q., et al. 2012, RAA, 12, 1197
da Cunha, E., Hopkins, A. M., Colless, M., et al. 2017, PASA, 34, e047
Dalcanton, J. J., Williams, B. F., Seth, A. C., et al. 2009, ApJS, 183, 67
Dalton, G., Trager, S., Abrams, D. C., et al. 2014, Proc. SPIE, 9147, 91470L
Dawson, K. S., Kneib, J.-P., Percival, W. J., et al. 2016, AJ, 151, 44
Dawson, K. S., Schlegel, D. J., Ahn, C. P., et al. 2013, AJ, 145, 10
de Jong, R. S., Barden, S., Bellido-Tirado, O., et al. 2014, Proc. SPIE, 9147, 91470M
Delubac, T., Bautista, J. E., Busca, N. G., et al. 2015, A&A, 574, A59
Delubac, T., Raichoor, A., Comparat, J., et al. 2017, MNRAS, 465, 1831
Dwelly, T., Salvato, M., Merloni, A., et al. 2017, MNRAS, 469, 1065
Eisenstein, D. J., Weinberg, D. H., Agol, E., et al. 2011, AJ, 142, 72
Filiz, Ak, N., Brandt, W. N., Hall, P. B., et al. 2014, ApJ, 791, 88
Freeman, K., Ness, M., Wylie-de-Boer, E., et al. 2013, MNRAS, 428, 3660
Frieman, J. A., Bassett, B., Becker, A., et al. 2008, AJ, 135, 338
Furnell, K. E., Collins, C. A., Kelvin, L. S., et al. 2018, MNRAS, submitted
Gilmore, G., Randich, S., Asplund, M., et al. 2012, Msngr, 147, 25
Goddard, D., Thomas, D., Maraston, C., et al. 2017, MNRAS, 466, 4731
Grier, C. J., Trump, J. R., Shen, Y., et al. 2017, ApJ, 851, 21
Gu, M., Conroy, C., Law, D., et al. 2017, ApJ, submitted (arXiv:1709.07003)
Gunn, J. E., Carr, M., Rockosi, C., et al. 1998, AJ, 116, 3040
Gunn, J. E., Siegmundr, W. A., Mannery, E. J., et al. 2006, AJ, 131, 2332
Holtzman, J. A., Shetrone, M., Johnson, J. A., et al. 2015, AJ, 150, 148
Hutchinson, T. A., Bolton, A. S., Dawson, K. S., et al. 2016, AJ, 152, 205
Ibarra-Medel, H. J., Sánchez, S. F., Avila-Reese, V., et al. 2016, MNRAS, 463, 2799
Ilbert, O., Arnouts, S., McCracken, H. J., et al. 2006, A&A, 457, 841
Jansen, F., Lumb, D., Altieri, B., et al. 2001, A&A, 365, L1
Jensen, T. W., Vivek, M., Dawson, K. S., et al. 2016, ApJ, 833, 199
Jones, A., Kauffmann, G., D'Souza, R., et al. 2017, A&A, 599, A141
Kaiser, N., Aussel, H., Burke, B. E., et al. 2002, Proc. SPIE, 4836, 154
Kelvin, L. S., Driver, S. P., Robotham, A. S. G., et al. 2012, MNRAS, 421, 1007
Kollmeier, J. A., Zasowski, G., Rix, H.-W., et al. 2017, arXiv:1711.03234
LaMassa, S. M., Glikman, E., Brusa, M., et al. 2017, ApJ, 847, 100
LaMassa, S. M., Urry, C. M., Cappelluti, N., et al. 2016, ApJ, 817, 172
Lang, D. 2014, AJ, 147, 108
Lang, D., Hogg, D. W., & Schlegel, D. J. 2014, arXiv:1410.7397
Laureijs, R., Amiaux, J., Arduini, S., et al. 2011, arXiv:1110.3193
Law, D. R., Cherinka, B., Yan, R., et al. 2016, AJ, 152, 83
Law, D. R., Yan, R., Bershady, M. A., et al. 2015, AJ, 150, 19
Li, N., & Thakar, A. R. 2008, CSE, 10, 18
Lin, L., Lin, J.-H., Hsu, C.-H., et al. 2017, ApJ, 837, 32
Linder, E. & SNAP Collaboration 2002, BAAS, 34, 97.02
MacLeod, C. L., Green, P. J., Anderson, S. F., et al. 2017, arXiv:1706.04240
Madrid, J. P., & Macchetto, D. 2009, BAAS, 41, 913
Majewski, S. R., Schiavon, R. P., Frinchaboy, P. M., et al. 2017, AJ, 154, 94
Margala, D., Kirkby, D., Dawson, K., et al. 2016, ApJ, 831, 157
McGraw, S. M., Brandt, W. N., Grier, C. J., et al. 2017, MNRAS, 469, 3163
Meisner, A. M., Lang, D., & Schlegel, D. J. 2017, AJ, 153, 38
Morganson, E., Green, P. J., Anderson, S. F., et al. 2015, ApJ, 806, 244
Myers, A. D., Palanque-Delabrouille, N., Prakash, A., et al. 2015, ApJS, 221, 27
Ness, M., Hogg, D. W., Rix, H.-W., Ho, A. Y. Q., & Zasowski, G. 2015, ApJ, 808, 16
Nidever, D. L., Holtzman, J. A., Allende Prieto, C., et al. 2015, AJ, 150, 173
Palanque-Delabrouille, N., Magneville, C., Yèche, C., et al. 2016, A&A, 587, A41
Pâris, I., Petitjean, P., Aubourg, E., et al. 2017b, A&A, in press (arXiv:1712.05029)
Pâris, I., Petitjean, P., Ross, N. P., et al. 2017, A&A, 597, A79
Perryman, M. A. C., de Boer, K. S., Gilmore, G., et al. 2001, A&A, 369, 339
Pinsonneault, M. H., Elsworth, Y., Tayer, J., et al. 2018, ApJS, submitted

Prakash, A., Licquia, T. C., Newman, J. A., et al. 2016, ApJS, 224, 34
Predehl, P., Andritschke, R., Becker, W., et al. 2014, Proc. SPIE, 9144, 91441T
Queiroz, A. B. A., Anders, F., Santiago, B. X., et al. 2018, MNRAS, 476, 2556
Raddick, M. J., Ani, R. T., Alexander, S. S., & Rafael, DC. S. 2014a, CSE, 16, 22
Raddick, M. J., Ani, R. T., Alexander, S. S., & Rafael, DC. S. 2014b, CSE, 16, 32
Raichoor, A., Comparat, J., Delubac, T., et al. 2016, A&A, 585, A50
Raichoor, A., Comparat, J., Delubac, T., et al. 2017, MNRAS, 471, 3955
Rockosi, C., Beers, T. C., Majewski, S., Schiavon, R., & Eisenstein, D. 2009, astro2010: The Astronomy and Astrophysics Decadal Survey, 2010
Ruan, J. J., Anderson, S. F., Cales, S. L., et al. 2016, ApJ, 826, 188
Runnoe, J. C., Cales, S., Ruan, J. J., et al. 2016, MNRAS, 455, 1691
Sako, M., Bassett, B., Becker, A. C., et al. 2014, arXiv:1401.3317
Salvato, M., Buchner, J., Budavári, T., et al. 2018, MNRAS, 473, 4937
Sánchez, S. F., Avila-Reese, V., Hernandez-Toledo, H., et al. 2017a, RMxAA, submitted (arXiv:1709.05438)
Sánchez, S. F., Barrera-Ballesteros, J. K., Sánchez-Menguiano, L., et al. 2017b, MNRAS, 469, 2121
Sánchez, S. F., Kennicutt, R. C., Gil de Paz, A., et al. 2012, A&A, 538, A8
Sánchez, S. F., Pérez, E., Sánchez-Blázquez, P., et al. 2016a, RMxAA, 52, 21
Sánchez, S. F., Pérez, E., Sánchez-Blázquez, P., et al. 2016b, RMxAA, 52, 171
Sánchez-Menguiano, L., Sánchez, S. F., Pérez, I., et al. 2016, A&A, 587, A70
Santiago, B. X., Brauer, D. E., Anders, F., et al. 2016, A&A, 585, A42
Saxton, R. D., Read, A. M., Esquej, P., et al. 2008, A&A, 480, 611
Schultheis, M., Zasowski, G., Allende Prieto, C., et al. 2014, AJ, 148, 24
Shen, Y., Brandt, W. N., Dawson, K. S., et al. 2015, ApJS, 216, 4
Shen, Y., Horne, K., Grier, C. J., et al. 2016, ApJ, 818, 30
Smee, S. A., Gunn, J. E., Uomoto, A., et al. 2013, AJ, 146, 32
Steinmetz, M., Zwitter, T., Siebert, A., et al. 2006, AJ, 132, 1645
Stoughton, C., Lupton, R. H., Bernardi, M., et al. 2002, AJ, 123, 485
Thakar, A. R. 2008, CSE, 10, 9
Thakar, A. R., Szalay, A., Fekete, G., & Gray, J. 2008, CSE, 10, 30
Voges, W., Aschenbach, B., Boller, T., et al. 1999, A&A, 349, 389
Wake, D. A., Bundy, K., Diamond-Stanic, A. M., et al. 2017, AJ, 154, 86
Wang, J., Shi, J., Pan, K., et al. 2016, MNRAS, 460, 3179
Weijmans, A.-M., Blanton, M., Bolton, A. S., et al. 2016, arXiv:1612.05668
Weijmans, A.-M. & MaNGA Team 2016, in Multi-Object Spectroscopy in the Next Decade: Big Questions, Large Surveys, and Wide Fields 507, 257 arXiv:1508.04314
Wilkinson, D. M., Maraston, C., Goddard, D., Thomas, D., & Parikh, T. 2017, MNRAS, 472, 4297
Wilkinson, D. M., Maraston, C., Thomas, D., et al. 2015, MNRAS, 449, 328
Yan, R., Bundy, K., Law, D. R., et al. 2016a, AJ, 152, 197
Yan, R., et al. 2017, arXiv:1708.04688
Yan, R., Tremonti, C., Bershady, M. A., et al. 2016b, AJ, 151, 8
Yanny, B., Rockosi, C., Newberg, H. J., et al. 2009, AJ, 137, 4377
York, D. G., Adelman, J., Anderson, J. E., Jr., et al. 2000, AJ, 120, 1579
Zacharias, N., Finch, C. T., Girard, T. M., et al. 2013, AJ, 145, 44
Zasowski, G., Cohen, R. E., Chojnowski, S. D., et al. 2017, arXiv:1708.00155
Zhao, G.-B., Wang, Y., Ross, A. J., et al. 2016, MNRAS, 457, 2377
Zhu, G. B., Barrera-Ballesteros, J. K., Heckman, T. M., et al. 2017, MNRAS, 468, 4494
Zucker, D. B., de Silva, G., Freeman, K., Bland-Hawthorn, J. & Hermes Team 2012, Galactic Archaeology: Near-Field Cosmology and the Formation of the Milky Way, 458, 421